Journal of Archaeological Science: Reports 32 (2020) 102436

Contents lists available at ScienceDirect

Journal of Archaeological Science: Reports

journal homepage: www.elsevier.com/locate/jasrep

Materials analyses of stone artifacts from the EBA to MBA Minoan Tholos tomb P at Porti, Greece (Crete), by means of Raman spectroscopy: Results and a critical assessment of the method

Georgia Flouda[a,*], Aggelos Philippidis[b], Antonios Mikallou[b,c], Demetrios Anglos[b,c]

[a] Heraklion Archaeological Museum, Greek Ministry of Culture and Sports, 2 Xanthoudidou St., GR 712 02 Heraklion, Crete, Greece
[b] Institute of Electronic Structure and Laser, Foundation for Research and Technology-Hellas (IESL-FORTH), P.O. Box 1385, GR 711 10 Heraklion, Crete, Greece
[c] Department of Chemistry, University of Crete, P.O. Box 2208, GR 710 03 Heraklion, Crete, Greece

ARTICLE INFO

Keywords:
Stone artifacts
Raman analysis
Funerary
Tholos tomb
Minoan Crete
Porti

ABSTRACT

Detailed analytical work based on mobile Raman microspectroscopy has been performed on a mortuary assemblage, comprising a group of 59 stone artifacts (vessels, implements and figurines) excavated in one of the richest burial sites in south-central Crete, Tholos tomb P at the Minoan site of Porti (ca. 2700–1700 BCE). Mineral identification was possible for over half of the objects examined and the results expand our understanding, originally obtained on the basis of visual and microscopic characterization of the objects. Patterns of variability in the stones investigated are correlated with the typological repertoire of the final products and compared with data from the neighboring site of Apesokari; further inferences on craft specialization issues are finally drawn. In all, the data obtained lead us to suggest that stone vessel manufacture at Porti was predominantly focused on the exploitation of local softstone outcrops. This hypothesis agrees with the current knowledge concerning the geological formation of the Asterousia area, on the northern fringes of which the site of Porti is located. In parallel, the capacity of mobile Raman microspectrometry to contribute to stone object characterization as regards their mineral composition is discussed along with advantages and limitations of the methodology followed. Raman analysis is preformed quickly, non-invasively, directly on the object and over several spots across its surface for probing heterogeneous mineral distributions. The mobile spectrometer permits measurements to be conducted on location, namely within the museum study facilities. A major limitation with respect to obtaining clean analytical information resulted from strong fluorescence emission observed in some of the measurements, which interfered with the Raman scattering signal. These emissions were attributed to organic materials present on the stone surface either as environmental contamination or as a result of previous, often undocumented, conservation treatments. Finally, the need to collect and thoroughly characterize local stone outcrops as well as archaeological stone objects has become evident and building a representative Raman spectral database will certainly facilitate future studies.

1. Introduction: archaeological background and study objectives

Stone artifacts constitute the second most common category of objects formally deposited within Minoan collective burial complexes or in the exterior funerary spaces, where mortuary and commemorative practices took place during the Prepalatial and Protopalatial period, roughly covering the third and early-second millennium BC. During this extended time-span, the island of Crete experienced profound socio-economic and political changes. This manifested itself in the rise of power structures of a heterarchical nature, such as factions or corporate groups which became the agents of technological and ideological innovations (Schoep, 2002, 107; Whitelaw, 2017); also, in the invention of writing and the first elaborate administrative system as well as in the foundation of the first palaces. In the case of south-central Crete, evidence from well-explored settlements datable to the earliest stages of this transformation is limited. To this end, the study of the mortuary arena is still our best source for exploring social differentiation and the creation of social identities within and/or across communities as well as the interaction between sites at a regional level (Relaki, 2012, 292, 295; Legarra Herrero, 2014; Caloi, 2015; Déderix, 2017, 6–7, fig. 1). In this framework, the conduct of formalized funerary rituals becomes most relevant. These rituals are mainly materialized through the clay and

* Corresponding author at: Department Head, Department of Prehistoric and Minoan Antiquities, Heraklion Archaeological Museum, Greece.
E-mail address: gflouda@culture.gr (G. Flouda).

https://doi.org/10.1016/j.jasrep.2020.102436
Received 19 December 2019; Received in revised form 31 May 2020; Accepted 10 June 2020

stone objects used in ceremonies associated with the primary burial and the secondary treatment of the human remains in the tholos cemeteries.

With regard to Prepalatial and Protopalatial stone artifacts which constitute our focus in this paper, archaeological research has so far concentrated mainly on their typological and comparative analysis (e.g. the seminal study by Warren, 1969; Bevan, 2007; Palio, 2003), patterns of deposition in cemeteries or within individual burial complexes (Legarra Herrero, 2011; Relaki and Tsoraki, 2017) as well as materiality and production workshops and techniques (Warren, 1967; Evely, 1993; Palio, 2008, 249–257). Methodologies of experimental archaeology have recently been employed in order to explore matters of technology (Morero 2016a; 2016b, 171–191), which may provide evidence for inferring possible object production and exchange networks in which Minoan communities participated. Nevertheless, we still lack a complete understanding of the Cretan geological outcrops exploited for the production of these stone vessels and the specific stone materials used, the latter being so far characterized qualitatively through macroscopic analysis of the object surface (for exceptions, see Lazzarini, 2001; Lazzarini et al., 2002; Flouda et al., 2012). This limited understanding impedes one from further exploring aspects related to the use of the landscape in Prepalatial and Protopalatial Crete, the transmission of specialized knowledge and the social context of technological and consumption patterns.

With this scope in mind, we have employed Raman analysis, based on a portable microspectrometer, in an effort to thoroughly investigate and characterize the mineral profile of 59 stone artifacts from Tholos tomb P at the Early Bronze Age (EBA) to Middle Bronze Age (MBA) site of Porti in the Mesara plain (Fig. 1). The broader context of this archaeometric project is the study and publication of the archaeological evidence from the tomb, which has yielded one of the richest burial assemblages in south-central Crete (Fig. 2) and was summarily published by the excavator, Stephanos Xanthoudides (1924). The interdisciplinary approach of the overall study integrates intra-site analysis with scientific methods for the investigation of numerous finds, including human remains, bronze daggers and utensils, stone and ceramic vessels, stone implements, sealstones and jewellery pieces, obsidian tools, clay, and stone figurines.

Fig. 2. General view of Tholos tomb P at Porti (photo by G. Flouda, 2015).

This paper introduces the methodology followed in the present investigation with emphasis on the findings of the Raman analysis performed on the stone objects. In brief, Raman spectroscopy is a widely

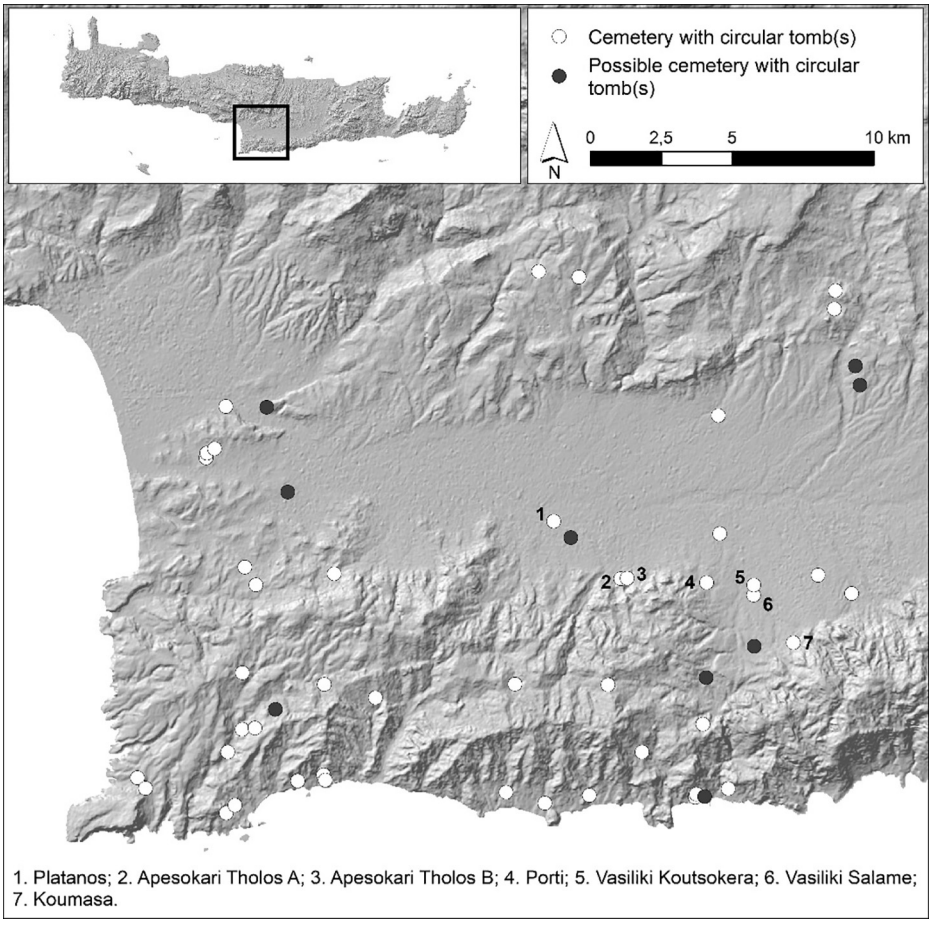

Fig. 1. Map of the Mesara Plain indicating the site of Porti (4) and other tholos tomb sites (courtesy of S. Déderix).

Table 1
Stone artifacts and brief analysis comments.

Heraklion Museum Inv. No	*Description*	*Image*	*Coloration of area(s) analyzed*	*Raman frequencies (cm^{-1})* [a]	*Identification* [a]
Γ172	figurine	Fig. 5; Xanthoudides, 1924, Pl. XXXIXb: 172	white	160, 286, 718, 1092	calcium carbonate ($CaCO_3$)
Γ173	figurine	Fig. 5; Xanthoudides, 1924, Pl. XXXIXb: 173	white/grey	160, 286, 714, 1092	calcium carbonate ($CaCO_3$)
Λ1038	palette	Fig. 13; Xanthoudides, 1924, Pl. XXXVIII: 1038	white	161, 287, 715, 1089	calcium carbonate ($CaCO_3$)
Λ1039	palette	Xanthoudides, 1924, Pl. XXXVIII: 1039	grey/white	165, 291, 718, 1094	calcium carbonate ($CaCO_3$)
Λ1040	palette	Xanthoudides, 1924, Pl. XXXVIII: 1040	grey/white	165, 291, 722, 1094	calcium carbonate ($CaCO_3$)
Λ1041	pallete	Xanthoudides, 1924, Pl. XXXVIII: 1041	grey/white	163, 289, 717, 1094	calcium carbonate ($CaCO_3$)
Λ1073	carinated bowl with a raised collar (MSV 8A)		grey	–	fluorescence
Λ1083	bowl (MSV 8B)	Xanthoudides, 1924, Pl. XXXVIII: 1083	grey/white	200, 677	steatite [$Mg_3Si_4O_{10}(OH)_2$]
Λ1075	bowl with carinated profile (MSV 8B, Warren 1969, P 111)	Xanthoudides, 1924, Pl. XXXVIII: 1075	black	196, 349, 438, 507	weak Raman signal (fluorescence)
Λ1078	carinated bowl with angular rim (MSV 8C)	Fig. 3; Xanthoudides, 1924, Pl. XXXIXa: 1078	green/white	97, 192, 259, 345, 695	–
Λ1071	carinated bowl with angular rim (MSV 8C)		grey	449, 610, 1117, 1293, 1415, 1529	titanium dioxide, rutile form (TiO_2) organic material
Λ1082	carinated bowl with angular rim (MSV 8C)		grey	196, 287, 345, 549	–
Λ1053	carinated bowl with angular rim (MSV 8C)	Xanthoudides, 1924, Pl. XXXIXa: 1053	dark grey	204, 291, 349, 450, 515	weak Raman signal (fluorescence)
Λ1345	carinated bowl with angular rim (MSV 8C)	Fig. 3	grey	156, 286, 718, 1092	calcium carbonate ($CaCO_3$)
Λ1054	miniature hemispherical bowl (MSV 8G)	Xanthoudides, 1924, Pl. XXXIXa: 1054	black	–	fluorescence
Λ1072	carinated bowl with a raised collar (MSV 8H, Warren, 1969, 206)	Fig. 3; Xanthoudides, 1924, Pl. XXXIXa: 1072	dark grey	1023, 1149	gypsum [$CaSO_4{\cdot}2H_2O$]
Λ1086	miniature bowl with carinated profile (MSV 8 I)		white/grey	149, 396	weak Raman signal (fluorescence)
Λ1070	deep carinated bowl (MSV 8 I)	Xanthoudides, 1924, Pl. XXXIXa: 1070	white	132, 199, 235, 348, 445, 597	weak Raman signal (fluorescence)
Λ4111	hemispherical bowl (MSV 8)		grey/white	286, 1089	calcium carbonate ($CaCO_3$)
Λ1049	bowl with three rim lugs and hook handle (MSV 10 A) Warren, 1969, 28, P 154)	Xanthoudides, 1924, Pl. XXXVIIIa: 1049	grey/white/ red/black	163, 286, 717, 1091	[all areas]: calcium carbonate ($CaCO_3$)
Λ1081	miniature bowl with rim lugs (MSV 10)	Xanthoudides, 1924, Pl. XXXVIIIa: 1081	grey/white/ blue	160, 286, 714, 1088	calcium carbonate ($CaCO_3$)
Λ1063	bowl (MSV 10A)	Xanthoudides, 1924, Pl. XXXVIIIa: 1063	white/yellow/brown	–	fluorescence
Λ1052	bowl with three rim lugs and handle (MSV 10A, Warren, 1969, 27)	Xanthoudides, 1924, Pl. XXXVIIIa: 1052	white/black	207, 294, 449, 518	weak Raman signal (fluorescence)
Λ1061	bowl with bow-shaped handle (MSV 10C, D 110, P 173)	Xanthoudides, 1924, Pl. XXXIVIIIa: 1061	black	–	fluorescence
Λ1048	bowl with staright stick handle (MSV 10C)	Xanthoudides, 1924, Pl. XXXVIIIa: 1048	grey	219, 360, 552, 673	indication for steatite ($Mg_3(Si_4O_{10})(OH)_2$)
Λ2089	polygonal bowl		red/black	284, 1089 156, 286, 1087, 1309, 1602	[red]: calcium carbonate ($CaCO_3$) [black]: calcium carbonate, black carbon
Λ1088	bird's nest bowl	Fig. 3	white/grey	137, 236, 388, 689	serpentinite (chrysotile form) [$(Mg_3(Si_2O_5)(OH)_4$]
Λ1065	bird's nest bowl	Fig. 3	grey	204, 373, 681	steatite [$Mg_3Si_4O_{10}(OH)_2$]
Λ1058	bird's nest bowl (unfinished)	Xanthoudides, 1924, Pl. XXXIXa: 1058	black	1336, 1592	black carbon
Λ1059	bird's nest bowl (unfinished)	Xanthoudides, 1924, Pl. XXXIXa: 1059	Brown	200, 349, 606, 1043	weak Raman signal (fluorescence)
Λ1087	bird's nest bowl	Fig. 3; Xanthoudides, 1924, Pl. XXXIXa: 1087	dark grey	144, 235, 445, 609, 1141, 1252, 1444	titanium dioxide, rutile form, (TiO_2), organic materials
Λ1084	bowl with straight stick handle (MSV 17A)	Xanthoudides, 1924, Pl. XXXVIIIa: 1084	green/grey	442, 609, 1106, 1284, 1407, 1522	titanium dioxide, rutile form, (TiO_2), organic materials
Λ1045	spouted bowl (MSV 17A)	Xanthoudides, 1924, Pl. XXXVIIIa: 1045	grey/green	163, 289, 1091, 372, 537, 824, 883	calcium carbonate ($CaCO_3$), andradite ($Ca_3Fe_2(SiO_4)_3$)
Λ 1050	miniature spouted bowl (MSV 17A)	Xanthoudides, 1924, Pl. XXXVIIIa: 1050	white	160, 286, 714, 1090	calcium carbonate ($CaCO_3$)
Λ 1044	handled bowl (or ladle?) (MSV 17 A, D131)	Xanthoudides, 1924, Pl. XXXVIIIa: 1044	grey	319, 619, 1373, 1428	–
Λ 1046	miniature bowl (MSV 17A, Warren, 1969, P 209)	Xanthoudides, 1924, Pl. XXXVIIIa: 1046	grey	141, 204, 295, 454, 1264	weak Raman signal (fluorescence)
Λ 1043	miniature bowl (MSV 17A, Warren, 1969, D 130, P 208)	Xanthoudides, 1924, Pl. XXXVIIIa: 1043	grey	143, 342, 609, 1292	weak Raman signal (fluorescence)
Λ 1042	miniature bowl (MSV 17A, Warren, 1969, D 129, P 207)	Xanthoudides, 1924, Pl. XXXVIIIa: 1042	grey	195, 348, 368, 510	weak Raman signal (fluorescence)

(*continued on next page*)

Table 1 (*continued*)

Heraklion Museum Inv. No	*Description*	*Image*	*Coloration of area(s) analyzed*	*Raman frequencies (cm^{-1})* [a]	*Identification* [a]
Λ1047	miniature bowl (MSV 17A, Warren, 1969, D 132, P 210)	Xanthoudides, 1924, Pl. XXXIXa: 1047	green/grey	237, 369, 595	weak Raman signal (fluorescence)
Λ1076	spouted bowl (MSV 17A)	Xanthoudides, 1924, Pl. XXXVIIIa: 1076	grey/white	286, 1091	[white]: calcium carbonate ($CaCO_3$)
Λ1064	miniature cup (MSV 17A, D 137, P 217)	Xanthoudides, 1924, Pl. XXXIXa: 1064	brown	–	fluorescence
Λ1069	carinated handled cup (MSV 17D). Similar with Λ 1055.	Xanthoudides, 1924, Pl. XXXIXa: 1069	white	160, 287, 714, 1092	calcium carbonate ($CaCO_3$)
Λ1055	deep hemispherical bowl (MSV 17D, Warren, 1969, 38, 40, D 140)		grey	133, 196, 349, 446, 511	weak Raman signal (fluorescence)
Λ2087	miniature jar with flaring sides (MSV 20B, Warren, 1969, 45, D157, P261)	Xanthoudides, 1924, Pl. XXXIXa: 2087	black/red	290, 1092	calcium carbonate ($CaCO_3$)
Λ1085	cylindrical jar (MSV 21A)		grey/white	159, 285, 713, 1087 158, 284, 712, 1086, 1281, 1407, 1525	[white]: calcium carbonate ($CaCO_3$) [grey]: calcium carbonate ($CaCO_3$), organic materials
Λ1062	stone cylindrical jar	Fig. 3; Xanthoudides, 1924, Pl. XXXIXa: 1062	dark grey/black	199, 356, 676	steatite [$Mg_3Si_4O_{10}(OH)_2$]
Λ1057	miniature cylindrical cup with Egyptian affinities (MSV 30D, Warren, 1969, D234, P426)	Fig. 3; Xanthoudides, 1924, Pl. XXXIXa: 1057	white/black	183, 305, 728, 1105 183, 305, 1105, 1311, 1605	[white]: dolomitic limestone [black]: dolomitic limestone, black carbon
Λ1066	miniature bowl (MSV 31A)		dark brown	207, 345, 453, 943	weak Raman signal (fluorescence)
Λ1067	shallow bowl (Warren, MSV 31A)		grey	163, 286, 771, 1091	calcium carbonate ($CaCO_3$)
Λ1342	stone miniature bowl (MSV 32A)	Xanthoudides, 1924, Pl. XXXVIIIa: 1342	green/white	282, 1088 140, 207, 352, 548	[white]: calcium carbonate ($CaCO_3$) [green]: -
Λ1077	shallow bowl (Warren, MSV 32A)	Xanthoudides, 1924, Pl. XXXVIIIa: 1077	grey/green/ white	166, 292, 1099 115, 210, 277, 363, 713	[white]: calcium carbonate ($CaCO_3$) [grey/green]: -
Λ1343	bowl (MSV 32 A, P442)		dark brown	326, 549, 1036, 1261, 1378, 1600, 1904, 2039	–
Λ1079	bowl (MSV 37B)		grey	1385, 1685	–
Λ1080	spouted bowl (MSV 37B)		green/white	–	fluorescence
Λ2086	teapot (MSV 41A, D 301, P 555)	Xanthoudides, 1924, Pl. XXXIXa: 2086	grey	–	fluorescence
Λ1056	miniature kernos (MSV 4D, D17, P52)	Xanthoudides, 1924, Pl. XXXIXa: 1056	black	1109, 1287, 1431	–
Λ2088	miniature alabastron with broken rim (MSV 1A, D 4, P 10)	Fig. 3; Xanthoudides, 1924, Pl. XXXIXa: 2088	dark grey	–	fluorescence
Λ1074	lid (MSV 27 I A)		grey	–	fluorescence
Λ1051	pyxis (MSV 33D)	Xanthoudides, 1924, Pl. XXXVIIIa: 1051; Bevan, 2007, 233: shape C33D	–		not analyzed
Λ1060	grinder	Xanthoudides, 1924, Pl. XXXIXa: 1060	grey	145, 392, 511, 628 461	titanium dioxide, anatase form (TiO_2), quartz

[a] Band frequencies are listed even in cases for which material identification was not inferred.

Fig. 3. Selection of stone vessels from Tholos tomb P on which Raman analysis was performed; top row, left to right: inv.nos. Λ2088, Λ1057, Λ1088, Λ1062, Λ1065; bottom row, left to right: inv.nos. Λ1087, Λ1078, Λ1345, Λ1072 (images by K. Sidiropoulos and G. Flouda).

employed method for materials analysis and has been shown to be a useful tool in the context of art conservation and archaeological science (Smith and Clark, 2004; Vandenabeele et al., 2007). The fundamental physical principle of Raman spectroscopy derives from the inherent property of molecular systems to scatter light. While the majority of the incident radiation is scattered elastically, maintaining its frequency (Rayleigh scattering), a very small fraction of it undergoes inelastic scattering, namely it alters its frequency as a result of its interaction (energy exchange) with the vibrational motions of the molecule. This inelastic scattering represents the Raman effect. The corresponding Raman spectra, obtained when the sample is illuminated by a monochromatic light source, typically a laser, convey information related to vibrations of the molecular bonding skeleton. These are known as vibrational modes and oscillate at specific frequencies, which manifest themselves in the form of distinct bands in the Raman spectra. These characteristic spectral bands serve as a fingerprint that enables identification of materials; in certain cases they allow discrimination of hardly distinguishable materials or even polymorphs of the same minerals (Smith, 2006; Colomban, 2012; Westlake et al., 2012; Baita et al., 2014). Progress in instrumentation has led to the development of mobile Raman spectrometers that facilitate significantly analytical campaigns in museums, monuments or excavation sites (Smith, 2006; Papliaka et al., 2016).

Major aim of the analytical investigation, described herein, has been first to provide a conclusive identification of the minerals in the stone artifacts and, ultimately, to lead to the expansion of the currently very limited body of data concerning the chemical/mineralogical characterization of the rocks. Patterns of variability in the stones investigated are correlated to the typological repertoire of the final products and further inferences on craft specialization issues are drawn. The impact of past, often poorly documented, conservation treatments of the archaeological material is also evaluated as a factor that potentially affects the efficiency of Raman analysis. Finally, the advantages and limitations of using mobile Raman spectroscopy for determining the raw materials and minerals of stone objects are also discussed.

2. The stone artifacts of Tholos tomb P at Porti: Patterns of production and consumption

Tholos tomb P, its rectangular annexes 'a-c', not preserved today, and a few individual pithos burials associated with them (Xanthoudides, 1924, 54–56, Pl. LXII; Legarra Herrero, 2014, 113) represent the cemetery of a Minoan site in the eastern part of the fertile Mesara plain, which stretches from the Bay of Mesara on the west to the Lasithi Mountains on the east (Fig. 2). The tholos belongs to the series of circular built tombs located in the northern foothills of the western Asterousia Mountains or at a short distance from them, including Apesokari Tholos A and B, Vasiliki Salame, Vasiliki Koutsokera, and Koumasa (Déderix, 2019, 159 fig. 1). Although the settlement of Porti has never been excavated (Xanthoudides, 1924, 54–55), its territorial extent has recently been traced through a field survey, the "Porti survey" (Alušík et al., 2019, 103–104). Notwithstanding the site having a secondary position within the regional communication network, the artifacts recovered from the tomb suggest that Porti had significant access to interregional exchange networks (Déderix, 2017, 18, 24). The tomb had been used for successive burials more or less continuously from the early Prepalatial up to the end of the Protopalatial period, which in terms of absolute chronology corresponds to ca. 2700–1700 BCE (see Shelmerdine, 2008, 3–7, fig. I.I, on Aegean relative and absolute chronology). In particular, a currently ongoing study of the material by G. Flouda suggests that the burial deposits date to the Early Minoan IIA through to the Middle Minoan II phases, while clay vessels excavated outside the tomb demonstrate that depositional activity continued at least until the early Neopalatial period (Middle Minoan IIIA phase). Three bridge-spouted burial pithoi were also excavated outside the tholos tomb and date probably from the late Protopalatial to the early Neopalatial period (Xanthoudides, 1924, 54–55, 62).

The understanding of mortuary practice, associated with Tholos tomb P, helps to reconstruct the choices made by the Porti community during the 3rd and early 2nd millennia BC and to approach interactions with other communities at the micro-scale. These parameters place the assemblage of the numerous stone vessels and the few stone implements and figurines, which together constitute the richest category of finds from Porti, into the foreground of our research focus.

From an archaeological perspective, the stone vessels from Porti are characterized by high variability in their shapes, especially when compared to similar assemblages from other Mesara sites (e.g. Evely, 2010; Gerontakou, 2003; Flouda, forthcoming). The assemblage comprises three main categories: drinking and offering vessels, miniaturized versions, and cosmetic containers (see Table 1, Fig. 3; also Table 2 for a chronological chart). Different size groups are represented, and the prevailing forms, classified according to the typology established by Warren (1969, *Minoan stone vases*, henceforward abbreviated as MSV), are the following:

1. Bowl with carinated profile (e.g. Λ1083, cf. MSV 8B).
2. Carinated bowl with angular rim (e.g. Λ1345, Λ1078, Λ1071, cf. MSV 8C) or with raised collar (e.g. vessel Λ1073, cf. MSV 8H, Warren, 1969, 23, 24). The group generally dates from EM IIB to MM I/II (Warren, 1969, 22; cf. also Relaki and Tsoraki, 2017,

Table 2
Chronological chart: Prepalatial to Neopalatial periods (adapted from Shelmerdine 2008, 3–7, fig. I.I).

Crete (Relative Chronology)	Absolute Chronology (Low)	Cyclades
Minoan Prepalatial Period		
Early Minoan I	3100–2700 BCE	Early Cycladic I (3100–2700 BCE)
Early Minoan IIA	2700–2400 BCE	
Early Minoan IIB	2400–2200 BCE	Early Cycladic II (2700–2200 BCE)
Early Minoan III	2200–2000 BCE	Early Cycladic III (2200–2000 BCE)
Middle Minoan IA	2000–1900 BCE	Middle Cycladic I (2000–1900 BCE)
Minoan Protopalatial Period		
Middle Minoan IB	1900–1800 BCE	Middle Cycladic II (1900–1700 BCE)
Middle Minoan II	1800–1700 BCE	
Minoan Neopalatial Period		
Middle Minoan III	1700–1600 BCE	Middle Cycladic III (1700–1590 BCE)
Late Minoan IA	1600–1500 BCE	
Late Minoan IB	1500–1450 BCE	

162–163 fig. 3).

3. Bowl with straight or hook handle (e.g. Λ1042 − 1047, Λ1076, Λ1064, cf. MSV 17A) or cup with vertical handle (e.g. Λ1064, cf. MSV 17B).
4. Bowl with rim lugs and handle (e.g. Λ1049, Λ1052, Λ1063, cf. MSV 10A; Warren, 1969, 27, also, Relaki and Tsoraki, 2017, 166).
5. Shallow bowl with bow-shaped or straight handle (e.g. Λ1048, cf. MSV 10C; Λ1084).
6. Shallow handless bowl (e.g. Λ1342, Λ1077, cf. MSV 32A; Λ1067, cf. MSV 31A).
7. Bird's nest bowl (e.g. Λ1088, Λ1065, Λ1058, Λ1087, cf. Warren, 1969, 10).
8. Miniature cylindrical jar with everted rim and base (e.g. Λ1057, cf. MSV 30 D, Warren, 1969, 74–76, D234, P426). A form imitating Egyptian prototypes of VIth to XIth Dynasty in date, and probably dating to MM IIB/MM III–LM III A1 (Warren, 1969, 74–76, D234, P426).
9. Cylindrical jar (e.g. Λ1085, cf. MSV 21 A; Λ1062). Warren (1969, 45) recognizes in this shape a common small funerary form of MM I, produced in a variety of materials, mostly in the Mesara, at the sites of Hagia Triada, Apesokari, Platanos, Koumasa, Kamilari, and Porti.
10. Miniature kernos (e.g. Λ1056, cf. MSV 4 D, D17, P426).

Based on stylistic dating criteria and on associations with pottery finds from the tomb, it is concluded that these vessels have most probably been manufactured within the period from EM IIB to MM II. It is not clear, though, how the variation in stone vessel forms and sizes correlates to patterns of production and consumption during the long use of Tholos tomb P at Porti for successive funerary events and associated rituals. This is due to the complete lack of evidence on settlement deposits from Porti and the neighboring sites, a factor that also poses limitations to our understanding regarding the use of these vessels. Nonetheless, comparanda from other sites provide insights into the formal repertoire of the Porti assemblage and its production. Particularly interesting, for example, is the fragmentary alabastron, inv.no. Λ2088 (Fig. 3), its circular inlay cutouts placing it into the "hatch-and-inlay group" (cf. Warren, 1969, 5, P10, D4 for its original form before breakage). A centre of production at Platanos has been postulated (Bevan, 2007, 91; also, Warren, 1969, 8-10), as two very similar alabastra have been excavated there (Xanthoudides, 1924, Pl. LIII: nos 1682–1683). Vessel Λ2088 from Porti can also be compared to the serpentinite vessel Λ2817 (SV19) from Apesokari Tholos A (Schörgendorfer, 1951, 20, Pl. 24.2), for which an early date has been suggested (Flouda, forthcoming).

As evidenced with most Prepalatial and Protopalatial tholos tombs, the periodic cleaning of the Tholos tomb P interior, which probably included the use of fumigation (Xanthoudides, 1924, 56), as well as the post-depositional treatment of the decomposed human remains and their disassociation from the original groups of grave goods, had the effect of muting individual identity and social distinctions in favour of the corporate identity of the community (Murphy, 2011, 38–41). The aforementioned burial practices have also blurred contextual associations, so inferences on the deposition of the vessels within the tomb in relation to individual burials are not possible. Moreover, stone vessels from burial contexts generally resist attempts of precise dating, since, as durable objects, they were often passed on as heirlooms from one generation to the next (Bevan, 2004, 107, 110, 112; Bevan, 2007, 157, 163; Girella, 2015, 246–247; Palio and Cucuzza, 2018). Accordingly, alternative pathways for the study of such objects concentrate on searching for the provenance of raw materials and the manufacturing techniques, which could provide evidence on craft specialization. To this end, one of the main goals of the work presented in this paper has been to explore these parameters based on chemical and mineralogical information obtained through systematic Raman analysis of the assemblage of stone artefacts excavated at Porti.

3. Raman analysis methodology

The project followed a Raman analysis-based methodological procedure already employed in a similar study of stone artifacts from the cemetery of Tholos tombs A and B at Apesokari and the neighboring habitation site, located a few kilometres away from our current research focus, Tholos Tomb P at Porti (Flouda, 2011; 2012; Flouda, forthcoming; Vavouranakis, 2015). Data acquired a few years ago, via Raman analysis of a wide set of stone artifacts from Apesokari, generated the first systematic dataset concerning the chemical/mineral composition of stone objects dating from the Prepalatial through to the Protopalatial period (Flouda et al., 2012; Tsikouras, forthcoming), since until then the method had only been used for the study of sealstones (Economou et al., 2010; unpublished paper by Barbara Borda, presented at the Cretological conference in 2016).

In total, 59 out of 60 published stone artifacts from Tholos Tomb P at Porti, comprising two stone figurines, vessels and implements, such as "palettes" and a stone grinder, were studied at the premises of the Heraklion Archaeological Museum by use of a compact mobile Raman spectrometer (Fig. 4). Stone vessel inv.no. Λ1068 could not be traced in the museum storeroom and, thus, was not analyzed, while figurine Γ171 has not been studied, because according to macroscopic observation it is not made of steatite, as had originally been suggested, but of ivory (Xanthoudides, 1924, 67, Pl. VIII: 171; Vasilakis, 2017, 292 fig. 4). A few more stone objects from the site were recently found in the Museum storeroom but they were not examined, as they still remain unpublished. Moreover, 11 mineral and stone samples from the collection of the Natural History Museum of Crete (henceforward NHMC) were used as reference materials. These included: marble, serpentinite, ophicalcite/calcite, diabase, steatite/talc, breccia, black/grey limestone, quartzite, chlorite schist, travertine and sandstone. They

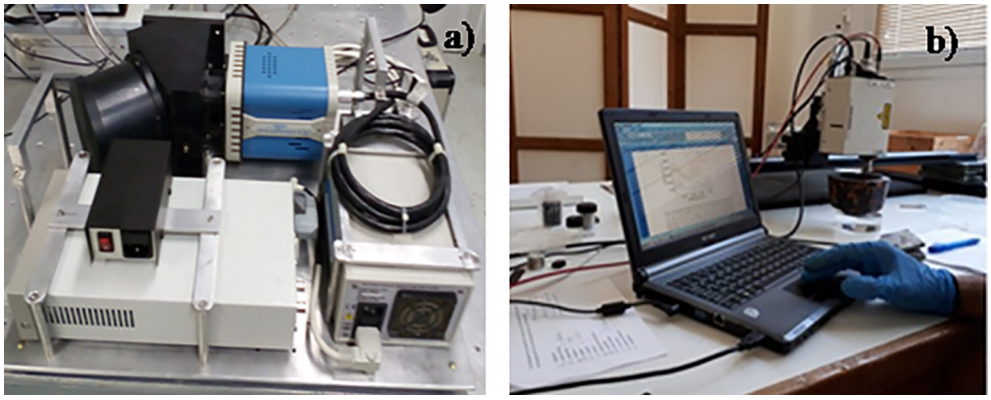

Fig. 4. a) Components of the mobile Raman spectrometer (spectrograph, detector, power supply unit) organized on a compact platform that fits in a carrying case, b) Image of the Raman system probe head during measurements at the Heraklion Archaeological Museum.

represent local lithologies, which have been classified by NHMC geologists, prior to the present study, by means of macroscopic examination. Raman analysis confirmed the mineral identity of the NHMC samples in almost all cases, and a corresponding set of reference spectra was acquired.

A mobile Raman microspectrometer (JY Horiba HE 785) was employed for the in-situ and non-invasive analysis of the stone artefacts. Excitation at 785 nm was provided by a cw (continuous wave) diode laser, coupled to an optical probe head that focusses the laser beam onto the sample surface by means of a set of objective lenses offering different levels of magnification. A white light-emitting diode (LED) and a digital colour camera are also included on the optical head and permit the operator to visualize the surface of the object and select the area (spot) to be analyzed. The scattered radiation is collected through the objective lens, passes through an edge filter that cuts off Rayleigh scattering, and via an optical fiber is fed into a compact spectrograph, equipped with a concave grating, which provides spectral coverage in the range of 120–3395 cm^{-1} at a spectral resolution of about 10–15 cm^{-1}. The detector, a Synapse CCD (1024 × 256 pixels), is Peltier-cooled and features high sensitivity with low dark counts. During the analysis of the stone objects, the power delivered by the laser beam on the sample surface was adjusted in the range of 3–30 mW. Typical exposure time for each scan on the CCD was 10–20 s, and spectra reported correspond to an average of 2 to 5 consecutive scans on the same point. All spectra presented are displayed as raw data with no subtraction of background. In certain cases, an offset has been applied to shift spectral curves vertically for clarity. The assignment of the observed Raman bands to specific vibrational modes and then to materials was facilitated via comparison against reference spectra of pure minerals or known samples, obtained in the context of this campaign or reported in the literature (Burgio and Clark, 2001, Smith and Clark, 2004) or given in open access databases such as http://rruff.info.

4. Results and discussion

Over the course of five days, corresponding to a total of 30 working hours, it became possible to analyze all 59 stone objects selected for the present analytical study. As already mentioned, several Raman spectra were collected for each object, at various points across its surface, in order to acquire a representative view of the main minerals present in the stone. The main findings obtained through Raman analysis are summarized in Table 1, where the objects are listed on the basis of their typology. For about half of the objects (32 out of 59) Raman analysis permitted straightforward identification of the dominant mineral or minerals providing important information on the stonework. Unfortunately, but not unexpectedly, fluorescence emission, attributed most likely to consolidants or coatings used during past object conservation work, interfered with the Raman scattering signal. Thus, in several cases Raman spectral bands were weak and superimposed over a broadband fluorescence background while in others intense fluorescence emission dominated the spectrum making it impossible to extract any useful analytical information from the recorded spectra, even though quite a few different points were examined across the surface of these objects. Also for a few of the objects, Raman spectra exhibited bands, in the region of 1000–1800 cm^{-1}, that were not obviously related to any relevant minerals and likely correspond to organic materials from past conservation treatments or surface contaminants related to object handling (Bordes et al., 2017).

Concerning the body of the 32 objects that afforded clean and conclusive Raman spectra, it turned out that they could be further categorized into two subgroups, based also on comparison with the reference geological samples. In subgroup A most of the objects (19) show Raman bands arising from calcium carbonate ($CaCO_3$) in the calcite form, which relates to either marble (metamorphic rock) or limestone (a carbonate sedimentary rock). In subgroup B (13 objects), minerals such as steatite, dolomitic limestone, serpentinite and titanium oxides (rutile/anatase) were identified. Indicative spectra obtained in the analysis of these objects are shown and discussed next.

Objects Γ172 and Γ173 (Fig. 5), two abstract anthropomorphic figurines, gave Raman spectra with bands at 160, 286, 718 and 1092 cm^{-1} corresponding to vibrational modes of calcium carbonate (Fig. 6). This result advocates for the hypothesis that these specific objects are most likely made of marble rock and this is further supported on the basis of macroscopic observation of the objects.

An interesting result is deduced from the analysis of the stone miniature cylindrical jar with Egyptian affinities, inv.no. Λ1057 (Fig. 3). More specifically, the distinct Raman bands at 183, 305, 728 and 1105 cm^{-1}, recorded when white colored areas of the object were analyzed correspond to dolomitic limestone, $CaMg(CO_3)_2$ (Fig. 7). This result confirms the identification of the stone through macroscopic observation (Warren, 1969, 76, D234, P426). It is also in agreement with a previous study of a stone implement from the area of Apesokari, in which mineral dolomite was also identified (Tsikouras, forthcoming). Surprisingly, when areas of black/dark coloration of the Porti jar were probed, Raman spectra showed a pair of broad bands attributed to black carbon (1311 and 1605 cm^{-1}), with those of limestone still present albeit weaker. Similarly, the Raman spectrum collected from one of the bird's nest bowls examined, inv.no. Λ1058, also presents the two broad bands in the range of 1300–1600 cm^{-1} corresponding to black carbon. This result is intriguing, however, it points clearly towards the presence of graphitic carbon, commonly produced under charring or combustion conditions, and thus forms strong evidence for exposure of the object to fire. Actually, in the present archaeological context, this hypothesis converges with the evidence for a burial stratum affected by fire inside the tholos, noted by the excavator (Xanthoudides, 1924, 56). In particular, this stratum consisted of earth mixed with bones blackened most

Fig. 5. Marble figurines, inv.no. Γ172 (left) and inv.no. Γ173 (right).

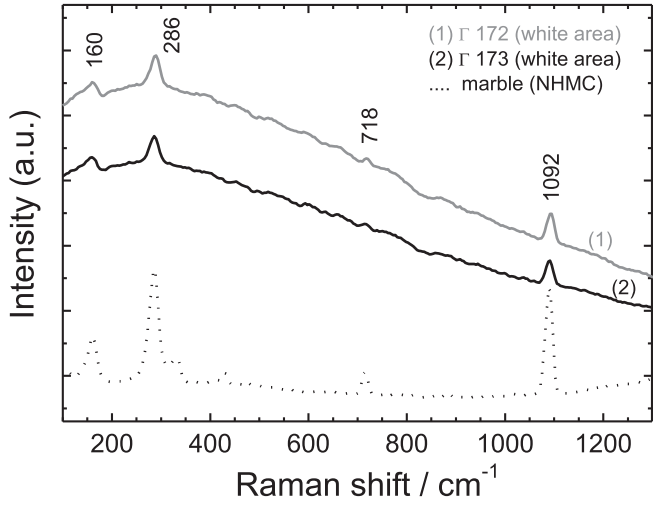

Fig. 6. Raman spectra collected from objects Γ172 (1) and Γ173 (2). A spectrum obtained from marble (NHMC mineral sample) is also shown as a reference (dotted line).

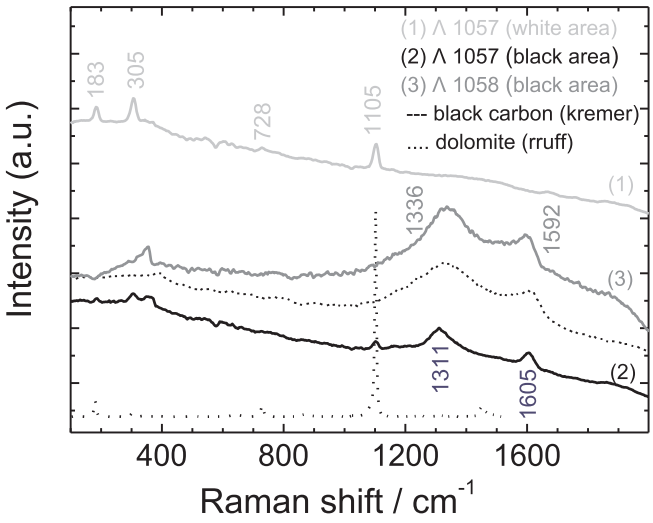

Fig. 7. Raman spectra from object Λ1057, recorded at a white (1) and a black coloured area (2) and object Λ1058, recorded at a black coloured area (3). Spectra of black carbon (Kremer Pigmente; dashed line) and dolomite (rruff; dotted line) are shown as reference.

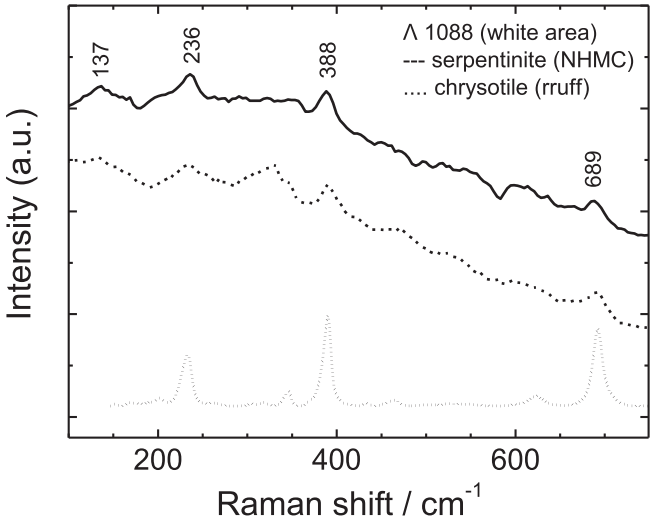

Fig. 8. Raman spectrum collected from object Λ1088 (white area) with the vibrational bands observed corresponding to chrysotile. A spectrum obtained from a serpentinite stone (NHMC; dashed line) and one of chrysotile (rruff; dotted line) are presented as reference.

likely because of exposure to a strong fire. Recent osteological studies from a number of Minoan cemeteries in Crete (e.g. Kamilari Tholos A, Livari-Skiadi tholos tomb, Moni Odigitria A and B, Kephala Petras Rockshelter) have advanced our knowledge on the burning of bones as a distinctive mortuary process (Triantaphyllou, 2016; 2018). The recently excavated lowest burial stratum of Koumasa Tholos B, a neighboring site of Porti, has also established that burning of human remains in high temperatures was practiced inside the tholos tombs (Panagiotopoulos, 2015, 235–236).

In the case of the stone bird's nest bowl, inv.no. Λ1088, the Raman spectrum, collected on a white area (Fig. 8), documents, on the basis of characteristic vibrational bands at 137, 236, 388 and 689 cm^{-1}, the presence of chrysotile ($Mg_3(Si_2O_5)(OH)_4$), a mineral of the serpentine group. It is well known that serpentinite is a metamorphic rock, mainly composed of serpentine group minerals, primarily chrysotile, antigorite and lizardite. These mineral polymorphs have the same stoichiometry, $Mg_3(Si_2O_5)(OH)_4$, however, they have different crystal structures which can be distinguished by Raman spectroscopy (Rinaudo et al., 2003).

A different type of metamorphic silicate rock, steatite ($Mg_3(Si_4O_{10})(OH)_2$), was identified in the case of two objects, inv.no. Λ1062 (cylindrical jar) and inv.no. Λ1065 (bird's nest bowl), on the basis of weak Raman bands at 199, 360 and 676 cm^{-1} that correlate well with those obtained from a reference sample of the talc mineral (Fig. 9). It is noted that in a number of stone vessels and implements from Tholos Tomb A, Apesokari, and from the nearby building on Vigla hill, steatite has been identified as the main mineral (Tsikouras, forthcoming).

On the other hand, the bird's nest bowl, inv.no. Λ1087, has provided a rather strange finding (Fig. 10). Analysis of a dark gray area on the object revealed Raman bands corresponding to the rutile form of titanium dioxide (TiO_2) with weak evidence for carbon as well. Analysis at a different area of the object gave Raman bands likely attributed to organic materials, which may be related to a conservation treatment (e.g. consolidant, glue). Considering the presence of titanium dioxide, it

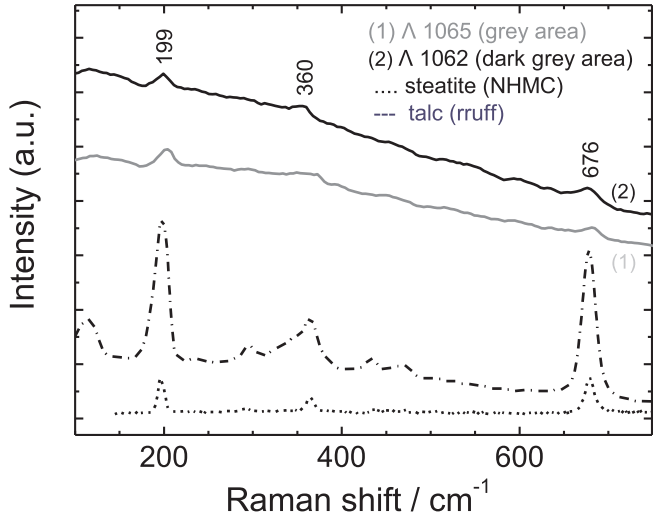

Fig. 9. Raman spectra from objects Λ1065 (1) and Λ1062 (2). A spectrum obtained from a sample of steatite mineral (talc form; NHMC) is shown as a reference (dotted line) along with one from talc (rruff; dashed line).

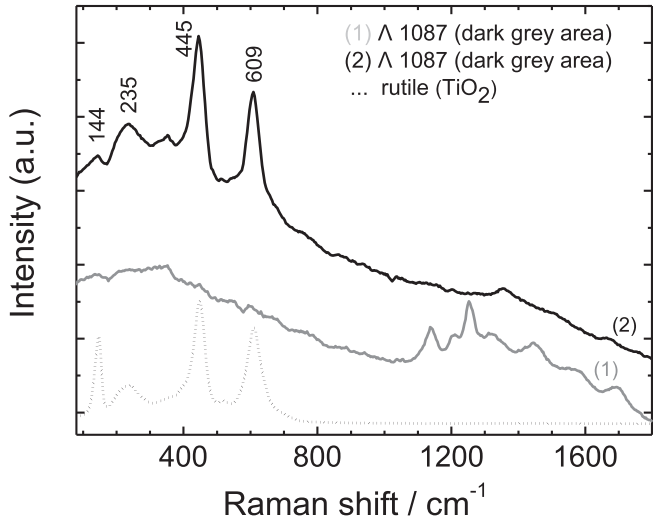

Fig. 10. Raman spectra collected from object Λ1087. The bands in the upper spectrum (2) correspond to titanium dioxide (rutile form, TiO_2) and the bands in the lower spectrum (1) are attributed to an organic material. A spectrum of pure rutile (Titanium dioxide, Sigma-Aldrich) is shown as a reference (dotted line).

is well known that rutile is an accessory mineral found in a variety of metamorphic and igneous rocks and this has also been shown through Raman spectral data (Meinhold, 2010; Prinsloo et al., 2011). Rutile was also identified in two more bowls, inv.nos Λ1071 and Λ1084. It is noted that a hypothesis concerning import of volcanic rocks from Santorini (Thera) as early as the Minoan period has been reported in the literature (Francaviglia, 1979) however no thorough investigation has been published to date as to the possibility that such volcanic stones may have been used to manufacture stone object as the ones investigated in the present study. A less probable scenario could attribute the detection of rutile on the stone objects to synthetic TiO_2 present in modern paints and conservation materials. Unfortunately, the absence of any documentation on conservation methods applied to objects excavated early in the 20th century, such as the ones in discussion, of commenting with higher certainty on the origin of both the organic materials and rutile on these objects.

Two of the stone bowls examined, inv.nos Λ1049 and Λ1078 (Fig. 3), were found to be composed of calcite ($CaCO_3$) and a still

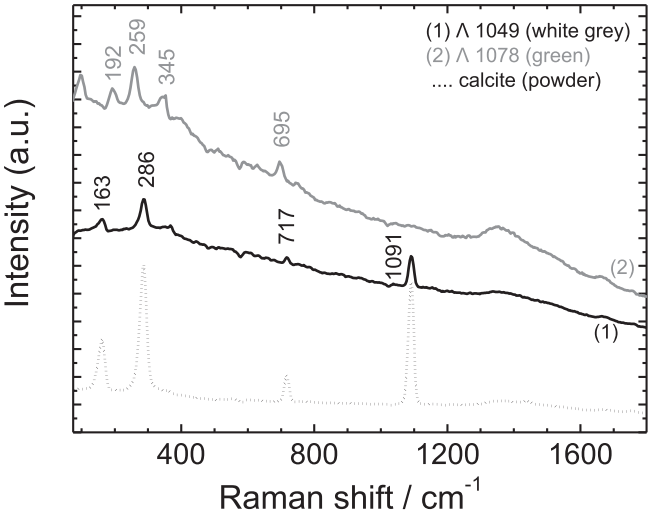

Fig. 11. Raman spectra obtained from objects Λ1049 (1) and Λ1078 (2). A spectrum from a sample of pure $CaCO_3$ in powder form (Calcium carbonate, Sigma-Aldrich) is shown as a reference (dotted line).

unidentified mineral or minerals, which however showed distinct Raman bands at 192, 259, 345 and 695 cm^{-1} most likely attributable to silicates (Fig. 11). Interestingly, Raman spectra from object Λ1049 showed no differentiation between the white/grey and dark blue/black areas analyzed.

The investigation of the stone grinder, inv.no. Λ1060, yielded weak Raman bands which are attributed mainly to the anatase form of titanium dioxide, TiO_2 (145, 392, 511, 628 cm^{-1}) and to quartz, SiO_2 (461 cm^{-1}) (Fig. 12). A plausible explanation, similar to that given earlier for rutile, is that anatase, a natural accessory rock mineral, may occur as inclusions in the stone (Smith, 2006; Wojcieszak and Wadley, 2019).

In the current study, six (6) of the stone artefacts examined, cannot be clearly characterized on the basis of the Raman spectra recorded. The main bands for this group of objects are tentatively attributed to organic materials with uncertainty as to whether they reflect the main constituent of the object, a superficial protective coating or a residue. It is noted that in a recent paper (Bordes et al., 2017) it has actually been pointed out that protein and fatty acid residues were identified on stone artefacts as a result of object handling during their study. Furthermore, for twelve (12) objects, because of strong fluorescence emission, the

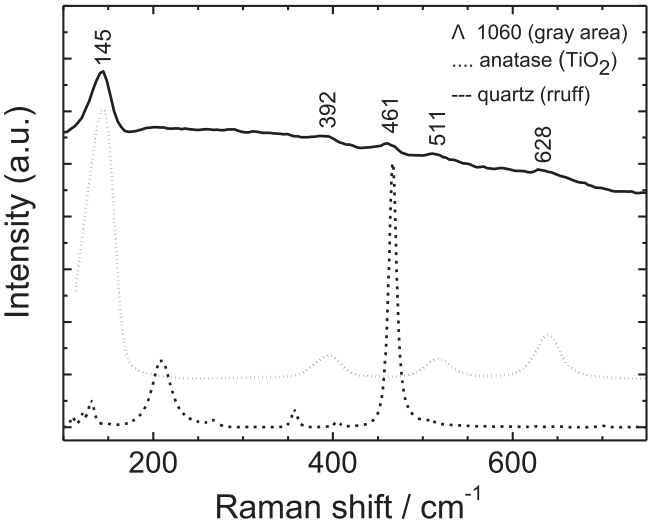

Fig. 12. Raman spectrum from object Λ1060 shown along with spectra of anatase, TiO_2 (Sigma-Aldrich; dotted line) and quartz (rruff; dashed line).

intensity of the Raman bands recorded in the spectra was quite low and only an indication could be provided as to the identity of the mineral. We present representative examples of these objects with the frequencies of the main Raman bands indicated for each one of them in Table 1.

Finally, for some of the objects (9), it was not possible to record meaningful Raman spectra as a result of the overwhelming broadband fluorescence emission which often was quite intense leading to saturation of the signal on the detector. The emission of fluorescence originates most likely either from superficial impurities accumulated or adsorbed over the course of the object's biography or from extraneous materials, such as coatings or consolidants, potentially used at the stage of conservation. It is noteworthy that all spectra obtained from the stone objects do show a broadband background, which implies that in most cases these organic contaminants interfere with the Raman scattering signal. Obviously this is an issue of concern, as it has a negative impact on one's capacity to acquire clean Raman spectra with high signal-to-noise ratio. In fact, a profound problem we encountered in this particular study has been the incomplete record of conservation procedure or procedures followed and the consolidants and structural adhesives used (e.g. epoxy resins), as the objects were excavated early in the 20th century. On the whole, the results of our study demonstrate that preservation practices may be one of the factors affecting the efficacy of the analytical method. Obviously, an analytical record documenting the use of coatings or consolidants during earlier conservation, could facilitate the choice of an appropriate solvent for removing organics before performing Raman measurements. Considering this lack of documentation, a fact that is not rare, an alternative approach to mitigating the problem would be to use of a Raman system with excitation at 1064 nm, known to minimize fluorescence emission.

5. Conclusions: Archaeological implications and prospective research advances

In conclusion, Raman analysis has led to a relatively accurate assignment of the main mineral identity for over half of the stone objects. The chemical composition for a number of stones relates to calcium carbonate, which can be further assigned to calcite, marble or limestone rock. For one of the stone vessels in this category, namely the carinated bowl, inv.no. Λ1345, it has been possible to macroscopically identify the raw material as calcite (Fig. 3), based on the fact that the stone is quite hard, mostly translucent, golden or honey brown with opaque creamy white patches (Warren, 1969, 128). The term calcite should hereby be differentiated from 'Egyptian alabaster' or 'calcite-alabaster' (Klemm and Klemm, 2008, 147–166), although no general agreement on the matter exists (Warren, 2017). From a typological point of view, the bowl belongs to a form linked to the Early Cycladic II Keros–Syros culture, ca. 2700–2300 BCE (Warren 1969, 27, P 154), which broadly parallels EM IIA and EM IIB (Kouka, 2009, 140 Table 7, 142 Table 9; Stampolidis and Sotirakopoulou, 2011b, 20; Wilson, 2008, 87). The choice of calcite as a raw material also for vessels, inv.no. Λ1049 and Λ1078 (Fig. 3), is justified by its working properties and its local availability. Since calcite reaches 3 on the Mohs scale of mineral hardness, it could be easily carved with knapped flint and an abrading stone as well as with the percussive use of metal chisels and points, tools also employed by craftsmen for the working of wood, ivory and bone (Bevan, 2012). For the same reason, calcite has been widely used for the production of sealstones during the Middle Minoan II (Krzyszkowska, 2018, 14–15).

The rest of the objects in the calcium carbonate group also comprise artifacts providing links with material from the Cyclades. The most interesting ones are the four stone rectangular palettes inv.nos Λ1038 – 1041 (Fig. 13) with a moulding on their flat upper surface (Xanthoudides, 1924, 64, Pl. XXXVIII), which find parallels to the palettes of the Early Cycladic I period (Bevan, 2004, 80–82, fig. 5.8:Cyc-4; Stampolidis and Sotirakopoulou, 2011a, 67). Their thick convex

Fig. 13. Stone palette, inv. no. Λ1038.

shape follows the type encountered mainly at the neighboring site of Koumasa (Xanthoudides, 1924, 15–16, Pl. XXI), and rather supports their possible use for pulverizing pigments, as well as mixing them during the burial rites for the purposes of body modification. Their examination with a digital microscope and penetrating light by Y. Maniatis and D. Tambakopoulos, following a technique employed extensively by them for measuring the crystallinity and determining the raw material of marble figurines from Crete (Tambakopoulos and Maniatis, 2007, 502–503 figs 2–5), has suggested that these palettes are most likely made of limestone. This finding resonates with the existence of local limestone resources near Porti, which have been substantiated by a small limestone quarry, recently traced about 150 m southwest of the hill where Tholos P is located, and probably exploited during the Roman period (Alušík et al., 2019a, 105–106, figs 7–20).

Another class of 'Cycladicizing' material are the two stone anthropomorphic figurines which are associated with Early Cycladic II types without reproducing their form (Stampolidis and Sotirakopoulou, 2011b, fig. 5a). Figurine inv.no. Γ172 (Fig. 5) has a featureless head and rectangular torso, the bottom part of which is elliptical. It belongs to the Cretan Porti type of schematic figurines (Branigan, 1971, 67, fig. 1.9; also, Ferrence, 2011, fig. 1c on a similar example from the cave of Hagios Charalambos), which resembles examples of the Cycladic Apeiranthos type (e.g. Marthari, 2017, 144–145 fig. 12.17: nos 1063, 3860 from Skarkos at Ios, Apeiranthos type, form 2). Figurine inv.no. Γ173 (Fig. 5) represents the indigenous Giophyrakia type (Branigan, 1971, 68, fig. 1.10). Both Porti figurines, inv.nos Γ172 and Γ173, are translucent at places and in our opinion they are most likely made of local marble. Naturally, tracing any systematic quarrying and exploitation of marble resources for the production of figurines during the Early Bronze age in Crete and in the Cyclades presents certain challenges (Tambakopoulos and Maniatis, 2017; Tziligkaki, 2007, 455). Durkin and Lister (1983) have reported the existence of white marble in the area of the Asterousia mountains but this suggestion has not been systematically pursued so far. Nonetheless, although it has been demonstrated that the use of marble at the site of Phaistos in western Mesara was rather restricted in comparison to limestone, chlorite and serpentinite, there have been 54 cases of marble objects identified

among a corpus comprising 900 stone vessels dating from the Prepalatial to the Protopalatial period (Palio, 2008, 25–26). It has also been pointed out that it has not always been possible to distinguish marble from limestone with certainty, although the macroscopic study and the results of a combination of thin-section petrography, X-ray diffractometry (XRD) and analysis of carbon and oxygen isotopes performed on a number of selected Phaistian vessels have also confirmed the presence of marble. It is noteworthy, though, that the analyses have led to the identification of a calcitic marble with grey veins as one of the rocks used (Lazzarini, 2001, 584, 586: CV 7, fig. 10; Palio 2008, 26, Pl. B.1–2); the minerals identified specifically include k-mica, plagioclase, rounded quartz, iron oxides and apatite. The marble outcrops in the area of Hagios Kyrillos/Dichali, close to the site where an EM III/MM IA tholos tomb and an associated settlement have been excavated, were suggested as the potential source of this marble (Lazzarini, 2002, 227; Tziligkaki, 2007, 455 n. 27). Besides, macroscopic study of the stone vessels from the three tholos tombs at Kamilari near Phaistos has also helped to identify one example of this particular local variety within four marble pieces in total (Caloi, 2019, 457 − 458 Table II.9.1). Furthermore, Tambakopoulos and Maniatis (2017, 512–513) also discuss a number of marble outcrops located near the site of Koumasa that lies close to Porti, in a gorge between Krotos and Koumasa, and, also, northwest of the village of Lendas. Importantly they point out that the marble resources at the latter site provide a white to whitish or greyish variety, well crystallised and at places with grey parallel veins, which is very similar to the Cretan figurines they ascribed as 'Type C'.

Based on this evidence, it is plausible to suggest that local limestone and marble resources were also exploited in the Mesara Plain for the manufacture of Cycladicizing figurines and artifacts, such as the discussed Porti examples. Besides, the interaction of Cretan communities with Cycladic material forms and practices and the emulation of Cycladic figurines and pottery wares, such as the imported Kampos Group, already started in the late EB I (ca. 2700 BCE), as shown by funerary contexts (Papadatos and Tomkins, 2013, 3). Since this emulation unfolded in different ways in trading or gateway-communities along north-central and eastern Crete, and at sites in south-central Crete (e.g. Carter, 1998, 71–73; Wilson, 2008, 82–84, 89–92), the parameter of raw material procurement and agency is an aspect of the production of Cycladicizing figurines and palettes, which needs to be addressed more systematically in the future through integrated archaeological and analytical studies.

In addition to the stone artifacts with chemical composition relating mainly to calcium carbonate, a second group of objects which consist of rocks such as steatite, dolomitic limestone and serpentinite was identified. An interesting example is the stone carinated bowl inv.no. Λ1072, which is most probably made of gypsum (Fig. 3). It belongs to a type broadly datable from EM IIB to MM I/II (type MSV 8H, cf. Warren, 1969, 206), and is comparable to vessel SV2 from Apesokari Tholos Tomb A (Warren, 1969, 22, 24, 218, cf. Type F) and to other examples from the Platanos cemetery (Xanthoudides, 1924, Pl. LIII: L1878; also, Gerontakou, 2003, 312 no. 27). The use of steatite for the manufacture of vessels inv.nos. Λ1065, Λ1062, 1083 and 1048, and of gypsum for vessel inv.no. Λ1072, respectively, complements our findings for the use of calcite at Porti. Both steatite and gypsum are soft stones, easy to drill, and relevant outcrops are available in central Crete (e.g. Gale et al., 1988, Gifford and Reese, 1995, 34 Table 3.2 on gypsum; Jones et al., 2007, 639–640 on steatite). On the other hand, it is possible that established perceptions of value also underlined the choice of steatite for vessels (Bevan, 2012, 8), since it was appreciated for its visual similarity to more precious materials, such as tarnished copper and silver due to its greenish and dark grey or bluish hues, respectively (Vickers and Gill, 1994, 105–153); the same may also be true for serpentinite. Indeed, copper and silver vessels were socially valued products during the Prepalatial and Protopalatial periods, because smelted ores of copper and silver had to be imported from Kythnos and Laurion as well as Siphnos, respectively (Stos-Gale and Gale, 2003), for them to be casted on Crete. However, this argument can only be sustained for stone vessels which presumably imitate metallic shapes, such as carinated bowls like inv.no. Λ1083 in the case of the Porti assemblage.

Another factor underlying the choice of steatite and gypsum as a raw material except from their material properties/affordance may have been the availability of local deposits. A thorough study on the characterization of steatite and related stones, based on an analytical protocol of Inductively-coupled plasma-mass spectrometry (ICP-MS) and Instrumental Neutron Activation Analysis (INAA) (Jones et al., 2007, 627, 639–640, Table 4b), has important implications for exploring this parameter. On the basis of the mineral compositional profile, as regards transition and rare earth metals, several steatite samples from Crete have been differentiated. Additional use of XRD analysis has significantly facilitated mineralogical analysis of steatite samples and further indicated four potential geological sources for steatite in central Crete, namely Spili, Gonies, Koxares and Miamou (Jones et al., 2007, 639–640). Hence, on the basis of its proximity to Porti, the Miamou site can be hypothesized as the source of raw materials for vessels inv.nos Λ1065, Λ1062, 1083 and 1048.

On the other hand, detailed macroscopic and petrographic analysis of gypsum decorative and architectural pieces from several archaeological sites and of samples acquired from outcrops has led to the classification of the gypsum varieties used and to their correlation with the archaeological finds (Chlouveraki, 2006, 238–240; Chlouveraki and Lugli, 2016). In Mesara, gypsum deposits relate to the laminated microcrystalline (balatino) type, in white to light brown hues, and have been traced at Haghia Triada, Ambelouzos, Roufas and Plouti-Moroni (Chlouveraki and Lugli, 2016, 663). Nonetheless, these and other sources in north Crete, such as Knossos Gypsades, have only been compared to the architectural gypsum pieces which have been analyzed. Therefore, the question whether the Mesara gypsum deposits might have been exploited for manufacturing stone vessels already by the Prepalatial and Protopalatial periods should be explored in the future through integrated studies of archaeological and geological examples.

On the whole, no clear pattern linking particular typological forms of vessels with a preference for specific raw materials emerged from our Raman analysis. The results presented herein confirm macroscopic observations and lead us to suggest that vessel industry on the site of Porti was predominantly focused on the exploitation of local softstone outcrops for manufacturing stone vessels. This hypothesis agrees with the preponderance of soft stones used at Phaistos (Palio, 2008, 26) and, also, with current knowledge on the geological setting of our study area. The tectonic sequence of Crete is characterized by a pile of thrust-nappes grouped in two major structural elements (Tortorici et al., 2012, 320–322, fig. 1: inset a, 332), i.e. upper and lower tectonic units, which are separated by a major shear zone (Chatzaras et al., 2006; Fassoulas et al., 1994; Jolivet et al., 1996; Seidel et al., 1982). The area of Porti is located in the geological formation of the metamorphic rocks of the Asterousia nappe (Fig. 14; Table 3) (Bonneau, 1972; Seidel et al., 1981), which constitutes part of the Uppermost tectonic unit (Rahl et al., 2004, 6–9, for a detailed review of Cretan geology; Tortorici et al., 2012, 323 fig. 3, for a structural sketch map of the western Asterousia mountains). This Uppermost tectonic unit is composed of a variety of rock types, including oceanic pillow basalts, gabbros, deep water marine sediments, amphibolites, schists, leucogranites, and an ophiolitic suite of mainly serpentinite (Rahl et al., 2004, 9 with further bibliography). Moreover, Porti also lies within a few kilometres from the Miamou nappe, which is part of the ophiolite-bearing mélange and tectonically underlies the Asterousia nappe (Bonneau et al., 1977), and within a rather close distance from the shallow marine carbonate rocks of the Tripolitza nappe, which flanks the Psiloritis mountain (Bonneau, 1984; Gifford and Reese, 1995, 32). Accordingly, most of the stones identified with our Raman analysis could easily have been acquired from the metamorphic and ophiolitic complexes of the wider region. An alternative hypothesis is that they were also collected as blocks or large

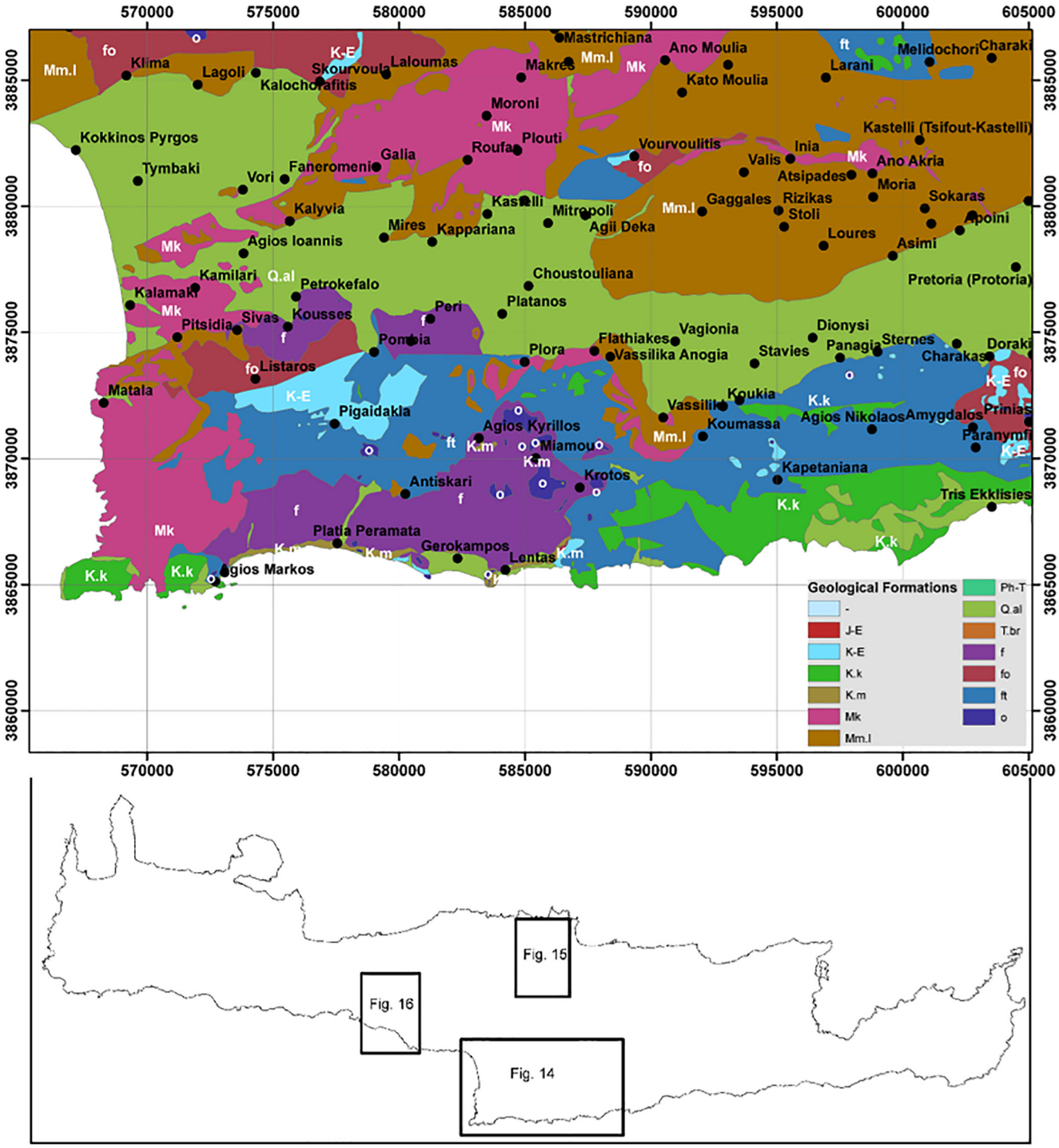

Fig. 14. Structural map of the wider study area (Mesara plain and Asterousia mountains) and map of Crete indicating the area shown (courtesy of A. Sarris). Legend: Table 3.

pebbles along the banks of the numerous streams that cut the narrow gorges of the Asterousia mountains (Palio, 2008, 25, Pl. B.10–11).

Furthermore, the presence of chrysotile ($Mg_3(Si_2O_5)(OH)_4$), a mineral of the serpentine group, documented by the Raman spectrum collected on a white area of the stone bird's nest bowl, inv.no. Λ1088, provides interesting associations. Since the variety of serpentinites in the Asterousia region consists entirely of antigorite (Koepke et al., 2002), the most probable source of the serpentinite at Porti appears to be the Philioremos outcrop near the village of Gonies west of Heraklion (Fig. 15; Table 3) or the areas of Spili and Ardachtos (Fig. 16; Table 3) northwest of the Mesara plain (Warren, 1969, 138–139; Athanasaki, 2014, 68, n. 22, Pl. XVIIIa; Grammatikakis et al., 2017, 8). Tsikouras (Tsikouras, forthcoming) has also reported the presence of lizardite and chrysotile in the case of stone objects from Tholos Tomb A at Apesokari based on Raman analysis.

Concerning the overall archaeological context, our analytical results provide interesting insights, when correlated to the Raman spectral data acquired for the stone artefacts from Tholos Tomb B at Apesokari. The latter have also been mostly manufactured out of soft stones, in contrast with the assemblage of stone vessels from Tholos A at the same site, which showed a preference for harder stones (Flouda et al., 2012, 47–48). This is probably justified by the earlier dating of Apesokari

Table 3
Types and corresponding codes for Geological Formations.

Geological Formations[a]	Codes
Allochthonous carbonate series	K.m
Pindos Zone carbonate rocks	K-E
Tripolis Zone carbonate rocks	K.k
Tripali Unit carbonate rocks	T.br
Plattenkalk Unit	J-E
Neogene formations	Mk
Neogene formations	Mm.I
Allochthonous Ophiolite complex	o
Quaternary formations	Q.al
Pindos Zone Flysch	fo
Tripolis Zone flysch	ft
Allochtonous flyschoid and schists formation	f
Phyllite-Quartzite series	Ph-T

[a] Source: http://emeric.ims.forth.gr/#cre8 (adapted from the maps of 'The Institute of Geology and Mineral Exploration (IGME) of Greece').

Tholos B and its assemblage, but it remains to be tested after full publication of the assemblage. Bevan (2012; 2007, 83, 88) notes that softstone traditions, such as the Early Bronze II Cretan and Cycladic ones, probably began by imitating wood- or ivory-working schemes into stone, mostly chlorite and steatite, as the skill-sets and tools required for each were very similar. On the other hand, stones of hardness above Mohs 3, for example the miniature cup, inv.no. Λ1057, made of dolomitic limestone (Fig. 3) with Mohs hardness of 3.5 to 4, must have demanded the use of more elaborate technologies. These were possibly a rock-hammer or toothless saw for roughing out the exterior, and some form of manual abrasion or drilling for removing the interior. Nonetheless, the use of drills at Porti needs to be systematically tested and reconstructed on the basis of the ongoing study of the stone vessels.

Furthermore, the future study of the artifacts from Porti Tholos P will also help to demonstrate their exact dating and to address the following questions: whether their production at an early stage is associated to the choice of the specific raw materials or whether this choice could relate to workshop traditions of different periods. In any case, the deduced prevailing use of soft stones did not demand a high

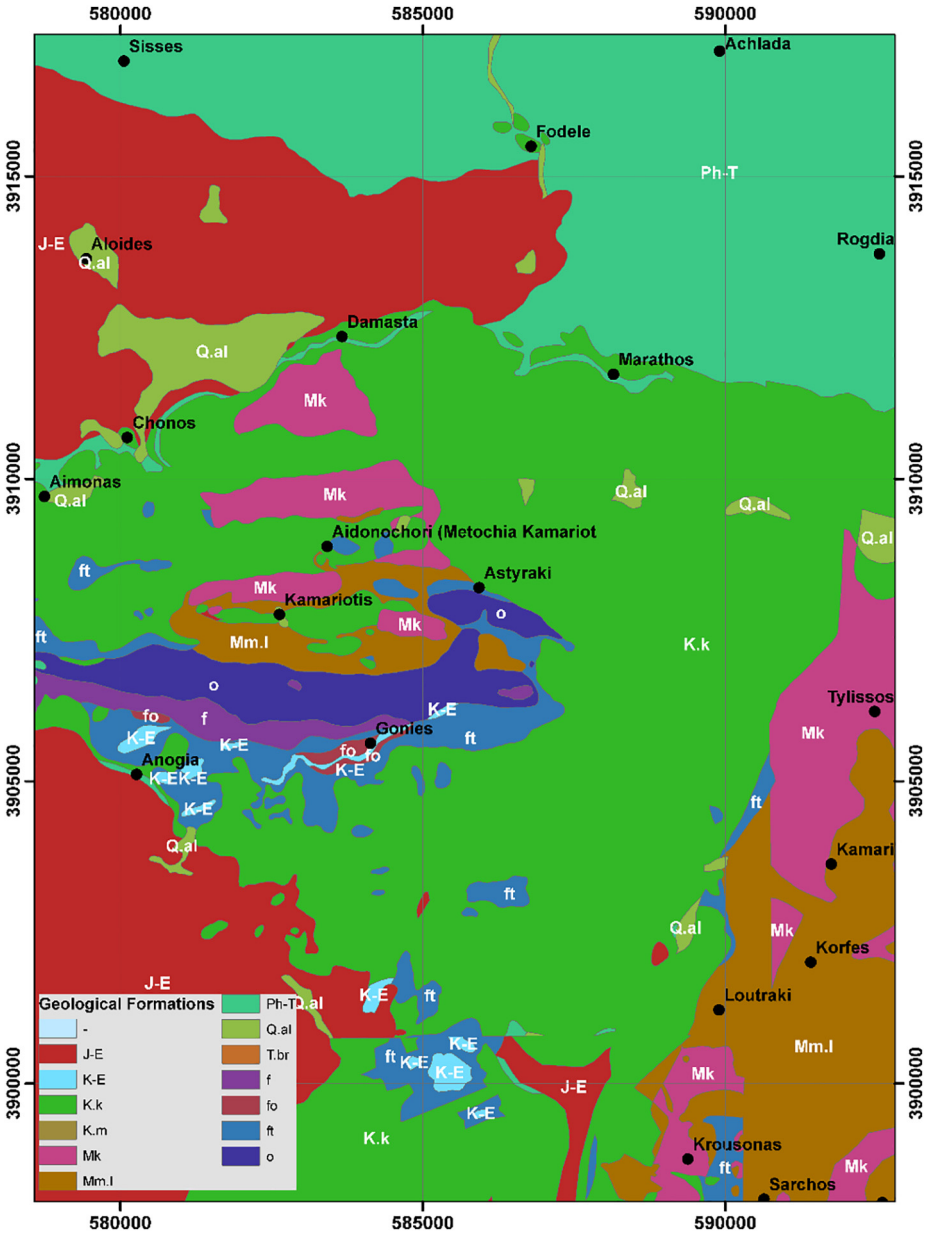

Fig. 15. Structural map of the area of Gonies (courtesy of A. Sarris); see Fig. 14 with map indicating the area shown. Legend: Table 3.

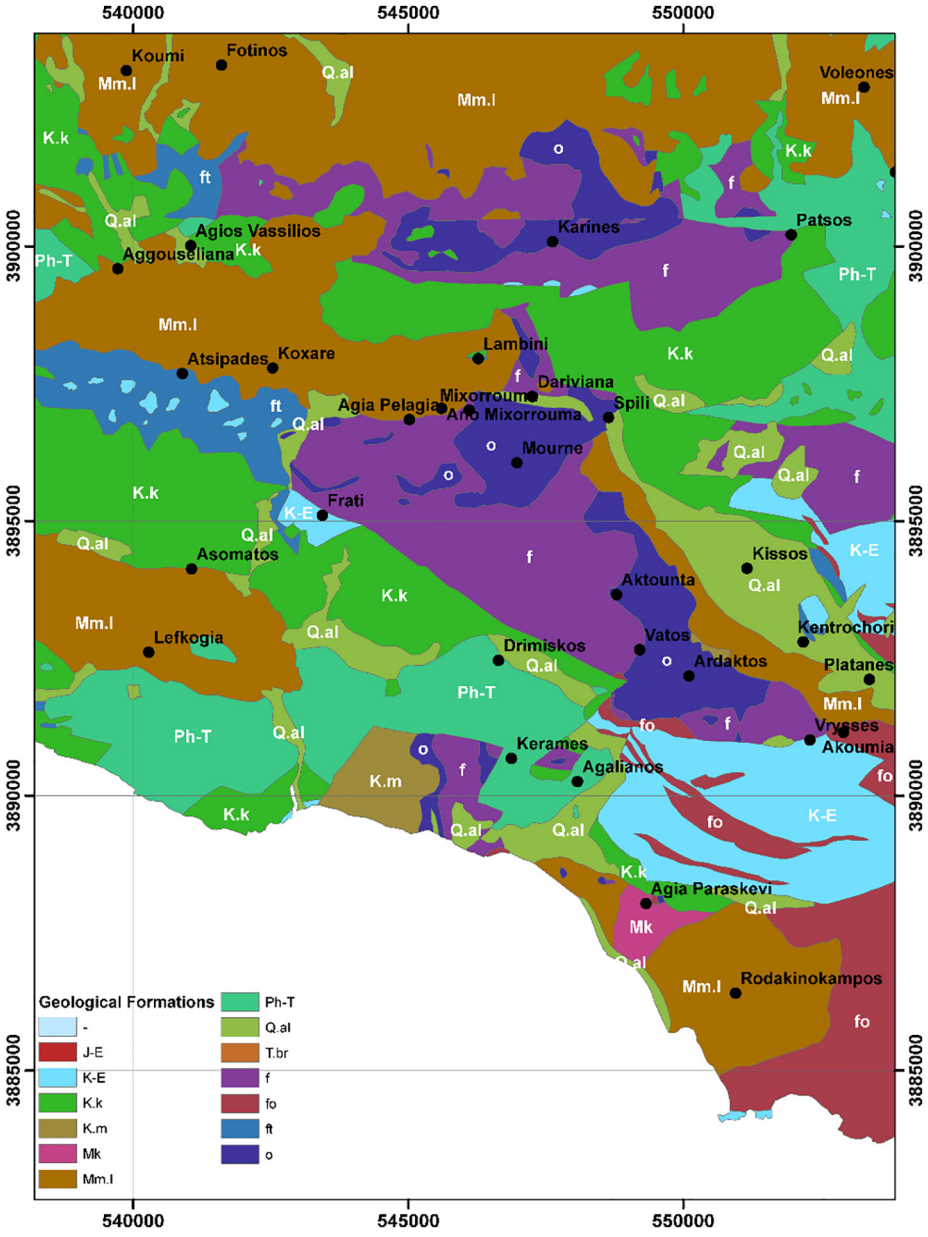

Fig. 16. Structural map of the areas of Spili and Ardachtos (courtesy of A. Sarris); see Fig. 14 with map indicating the area shown. Legend: Table 3.

degree of craft specialization, since the procurement of the raw materials was fairly simple, and the technique employed for manufacture was mostly carving with tools.

From a methodological point of view, Raman microspectroscopy, a non-invasive technique, has a high potential concerning the analytical investigation of stone objects. The mobile spectrometer permits measurements to be conducted on location, namely in the museum or at an archaeological site and, thus, has implications for curation practices. Measurements are performed quickly (within a few minutes) directly on the object, typically at several spots across its surface, and this is particularly important when stones of heterogeneous mineral distribution are studied. Raman spectra provide analytical information on both crystalline and amorphous materials. For example, calcite and aragonite, two different mineral structures of $CaCO_3$ can be differentiated on the basis of their Raman spectra and likewise two different phases of TiO_2, rutile and anatase. On the other hand, Raman analysis alone is not a decisive means to enable one to distinguish between marble and limestone. So in such a case, observation under the optical microscope may give complementary information aiding one to discriminate limestone from marble. As evidenced in this study, and widely known, a not uncommon limitation with Raman spectroscopy emerges when strong fluorescence is emitted, most likely originating from superficial contaminants related to burial or environmental deposits or from materials used during past, often undocumented, conservation treatments.

In all, an effective approach, based on Raman analysis for studying archaeological stone finds, requires a thorough investigation of many representative samples from local stone outcrops. This will help accumulate a broad spectral database that can be used for properly characterizing stone mineral profiles and furthermore inferring insights into the procurement routes of raw materials for the production of the stone vessels. As the issue of sourcing the stones is of high priority and great interest, it often becomes necessary to employ complementary analytical techniques some of which might require sampling. The optimal strategy in this context would be to make first a screening of objects by use of non-destructive mobile Raman, potentially with additional help from portable X-ray fluorescence (XRF) spectroscopy analysis. Then, selecting a narrow set of artifacts among the original assemblage, on the basis of targeting key analytical questions, one could move on with

using (micro) destructive techniques, such as XRD, after the relevant permits are granted. As already discussed, XRD has been used in combination with thin-section petrography and isotope analysis of carbon and oxygen isotopes for the investigation of Prepalatial/Protopalatial stone vessels from Phaistos (Lazzarini, 2001). However, both techniques, are invasive and according to the current specifications set by the Greek Ministry of Culture a permit for microsampling is not granted for whole artifacts.

CRediT authorship contribution statement

Georgia Flouda: Conceptualization, Methodology, Project administration, Writing - original draft, Writing - review & editing. **Aggelos Philippidis:** Methodology, Investigation, Formal analysis, Writing - original draft, Writing - review & editing. **Antonios Mikallou:** Investigation, Formal analysis. **Demetrios Anglos:** Methodology, Formal analysis, Validation, Writing - original draft, Writing - review & editing.

Acknowledgements

This research has been supported in part by: a) the "HELLAS-CH" project (MIS-5002735) implemented under the "Action for Strengthening Research and Innovation Infrastructures", funded by the Operational Programme "Competitiveness, Entrepreneurship and Innovation" (NSRF 2014-2020) and co-financed by Greece and the European Union (European Regional Development Fund) and b) the IPERION-CH project, funded by the European Commission, H2020-INFRAIA-2014-2015, Grant No. 654028. Ch. Fassoulas, head of the biodiversity department at NHMC is warmly thanked for providing the group of reference samples. We are also grateful to V. Tsikouras for helpful discussions and feedback concerning the mineralogy of the stones examined, to S. Sotiropoulou for discussions on the interpretation of selected Raman spectra and to Y. Maniatis and D. Tambakopoulos for examining the palettes, inv.nos Λ1038-1040, with optical microscopy. Many thanks are also directed to K. Sidiropoulos who photographed the stone vessels shown in Figure 3, to S. Déderix who has generated the map shown Figure 1 and to A. Sarris who has provided the geological formation maps shown in Figures 14–16.

References

Alušík, T., Vasilakis, A., Semerád, M., 2019. The Porti-Miamou project: 2015 season preliminary report and a report on an ancient quarry. In: Trefný, M. (Ed.), Colloquia classica. Proceedings from the 1st and 2nd year of the conference held on 29/06/2016 in Hradec Králové and on 27/06/2017 in Prague. Karlovy Vary - Stará Role, pp. 100–121.

Athanasaki, K., 2014. A Serpentine Quarry-Scape in Gonies, North-Central Crete. In: Touchais, G., Laffineur, R., Rougemont, F., (Eds.), PHYSIS. L'environnement naturel et la relation homme-milieu dans le monde Égéen Protohistorique. Actes de la 14e Rencontre égéenne international, Paris, Institut National d'Histoire de l'Art (INHA), 11 – 14 Dècembre 2012 (AEGAEUM 37). Peeters, Liége, pp. 67 – 72.

Baita, C., Lottici, P.P., Salvioli-Mariani, E., Vandenabeele, P., Librenti, M., Antonelli, F., Bersani, D., 2014. An integrated Raman and petrographic characterization of Italian mediaeval artifacts in pietra ollare (soapstone). J. Raman Spectrosc. 45, 114–122; doi.org/10.1002/jrs.4414.

Bevan, A., 2004. Emerging Civilized Values? The Consumption and Imitation of Egyptian Stone Vessels in EMII-MMI Crete and Its Wider Eastern Mediterranean Context. In: Barrett, J.C. and Halstead, P. (Eds.), The Emergence of Civilization Revisited. Oxford, UK, pp. 107–126.

Bevan, A., 2007. Stone vessels and Values in the Bronze Age Mediterranean. Cambridge University Press, Cambridge.

Bevan, A., 2012. Wood-Worked and Metal-Shocked: Softstone Vessels in the Bronze and Early Iron Age Eastern Mediterranean. In: Phillips, C., Simpson, S., (Eds.), Softstone in Arabia and Iran. Archaeopress, Oxford.

Bonneau, M., 1972. Existence d'un lambeau de cristallin chevauchant sur la série du Pinde en Crète moyenne (Grèce). Comptes rendus de l'Académie des sciences Paris 274, 2133–2136.

Bonneau, M., 1984. Correlation of the Hellenide nappes in the south-east Aegean and their tectonic reconstruction. In: Dixon, J.E., Robertson, A.H.F. (Eds.), The Geological Evolution of the Eastern Mediterranean. Geol. Soc. London, Spec. Publ., 17, pp. 517–528.

Bonneau, M., Angelier, J., Epting, M., 1977. Réunion extraordinaire de la Societé Géologique de France en Crete. Bull. Soc. Géol. Fr. 19, 87–102.

Bordes, L., Prinsloo, L.C., Fullagar, R., Sutikna, T., Hayes, E., Jatmiko, Saptomo E.W., Tocheri, M.W., Roberts, R.G., 2017. Viability of Raman microscopy to identify micro-residues related to tool-use and modern contaminants on prehistoric stone artefacts. J. Raman Spectrosc. 48, 1212–1221. https://doi.org/10.1002/jrs.5202.

Branigan, K., 1971. Cycladic Figurines and their derivatives in Crete. Ann. Br. School at Athens 66, 57–78. https://doi.org/10.1017/S0068245400019110.

Burgio, L., Clark, R.J.H., 2001. Library of FT-Raman spectra of pigments, minerals, pigment media and varnishes, and supplement to existing library of Raman spectra of pigments with visible excitation. Spectrochim. Acta A 57, 1491–1521. https://doi.org/10.1016/S1386-1425(00)00495-9.

Caloi, I., 2015. Recreating the past. Using tholos tombs in Protopalatial Mesara. In: Cappel, S., Günkel-Maschek, U., Panagiotopoulos, D. (Eds.), Minoan Archaeology. Perspectives for the 21st Century. Presses Universitaires de Louvain, Louvain-la-Neuve, pp. 255–266.

Caloi, I., 2019. I vasi di pietra. In: Girellla, L., Caloi, I., Kamilari. Una necropoli di tombe a tholos nella Messarà (Creta) (Monografie della Scuola Archeologica di Atene e delle Missioni Italiane in Oriente XXIX). Scuola Archeologica di Atene, Athens, pp. 457 – 484.

Carter, T., 1998. Reverberations of the "International Spirit": Thoughts upon "Cycladica" in the Mesara. In: Branigan, K. (Ed.), Cemetery and Society in the Aegean Bronze Age (Sheffield Studies in Aegean Archaeology 1). Sheffield Academic Press, Sheffield, pp. 59–77.

Chatzaras, V., Xypolias, P., Doutsos, T., 2006. Exhumation of high-pressure rocks under continuous compression: a working hypothesis for the southern Hellenides (central Crete, Greece). Geol. Mag. 143, 859–877. https://doi.org/10.1017/S0016756806002585.

Chlouveraki, S., 2006. Gypsum in Minoan Architecture: Exploitation, Utilisation and Weathering of a Prestige Stone. PhD thesis. University College London.

Chlouveraki, S., Lugli, S., 2016. Gypsum: A jewel in Minoan palatial architecture; identification and characterisation of its varieties. In: Maniatis, Y. (Ed.), Proceedings of the 7th International Conference of ASMOSIA, Thassos Greece, 15-20 September 2003 (BCH Suppl. 51), pp. 657–668.

Colomban, P., 2012. The on-site/remote Raman analysis with mobile instruments: a review of drawbacks and success in cultural heritage studies and other associated fields. J Raman Spectrosc. 43, 1529–1535. https://doi.org/10.1002/jrs.4042.

Déderix, S., 2017. Communication Networks, Interactions and Social Negotiation in Prepalatial South-Central Crete. Am. J. Archaeol. 121, 5–37. https://doi.org/10.3764/aja.121.1.0005.

Déderix, S., 2019. Patterns of Visibility, Intervisibility and Invisibility at Bronze Age Apesokari (Crete). Open Archaeol. 5, 187–203. https://doi.org/10.1515/opar-2019-0014.

Durkin, M.K., Lister, C.J., 1983. The Rods of Digenis: An Ancient Marble Quarry in Eastern Crete. Ann. Br. School at Athens 78, 69–96. https://doi.org/10.1017/S0068245400019663.

Economou, G., Konstantinidi-Syvridi, E., Kougemitrou, I., Perraki, M., Smith, D.C., 2010. A Mineralogical Study of some Mycenaean Seals employing mobile Raman Microscopy. Bull. Geol. Soc. Greece 43, 804–811. https://doi.org/10.12681/bgsg.11246.

Evely, R.D.G., 1993. Minoan Crafts: Tools and Techniques - An Introduction. Paul Åströms, Göteborg.

Evely, D., 2010. Stone vases and tools. In: Vasilakis, A., Branigan, K., Moni Odigitria. A Prepalatial Cemetery and Its Environs in the Asterousia, Southern Crete. INSTAP Academic Press, Philadelphia, pp. 171–185.

Fassoulas, C., Kilias, A., Mountrakis, D., 1994. Postnappe stacking and exhumation of high pressure/low-temperature rocks in the island of Crete, Greece. Tectonics 13, 127–138. https://doi.org/10.1029/93TC01955.

Ferrence, S., 2011. Variety is the spice of life: Figurines from the cave of Hagios Charalambos. In: Andreadaki–Vlazaki, M., Papadopoulou, E. (Eds.), Proceedings of the 10th International Cretological Congress, Chania, 1–8 October 2006, Vol. A3, pp. 597–611.

Flouda, G., 2011. Reassessing the Apesokari A tholos funerary record: preliminary thoughts. Rivista di Archeologia XXXV 111–121.

Flouda, G., 2012. Tholos tomb A at Apesokari/Mesara. In: Andrianakis, M., Varthalitou, P., Tzachili, I. (Eds.), Archaeological Work in Crete 2. Proceedings of the 2nd Meeting, Rethymnon, 26-28 November 2010. Rethymnon, pp. 132–143.

Flouda, G., forthcoming. An archaeological palimpsest. Tholos Tomb A and Habitation at Apesokari Mesara. INSTAP Academic Press, Philadelphia, USA.

Flouda, G., Vavouranakis, G., Katsaros, Th., Ganetsos, Th., Tsikouras, B., 2012. Non-destructive investigation using Raman spectroscopy of stone archaeological artefacts from Apesokari-Crete (Greece). In: Radvan, R., Akyuz, S., Similcanu, M., Dragomir, V. (eds.), Proceedings of The Third Balkan Symposium on Archaeometry. The Unknown Face of the Artwork, 29-30 October 2012. Bucharest, pp. 45–51.

Francaviglia, V., 1979. Volcanic rocks from Thera (Santorini) identified on Crete. Archeologia Classica 31, 273–285.

Gale, N.H., Einfalt, H.C., Hubberten, H.W., Jones, R.E., 1988. The sources of Mycenaean gypsum. J. Archaeol. Sci. 15, 57–72. https://doi.org/10.1016/0305-4403(88)90019-2.

Gerontakou, E., 2003. Δύο Μεσομινωικοί Αποθέτες του Πλατάνου. In: Vlachopoulos, A., Birtacha, K. (Eds.), Argonautes. Studies Presented to Professor Christos Doumas. I Kathimerini, Athens, pp. 303–330.

Gifford, J.A., Reese, D.S., 1995. The Physical Geology of the Western Mesara and Kommos. In: Shaw, J.W., and Shaw, M.C. (Eds.), Kommos: An Excavation on the South Coast of Crete, Volume I, Part I. The Kommos Region and Houses of the Minoan Town. Princeton University Press, Princeton, pp. 30–90.

Girella, L., 2015. Minor Objects. In: Karetsou, A., Girella, L., Kalochoraphitis. Two

chambers tombs from the LM IIIA2 – B cemetery. A contribution to postpalatial funerary practice in the Mesara. Bottega d' Erasmo – Aldo Ausilio Editore, Padova, pp. 235 – 256.
Grammatikakis, I., Demadis, K.D., Kyriakidis, E., Cabeza, A., Leon-Reina, L. 2017. New evidence about the use of serpentinite in the Minoan architecture. A μ-Raman based study of the "House of the High Priest" drain in Knossos. J. Archaeol. Sci. Rep 16, 316 – 321; doi.org/10.1016/j.jasrep.2017.09.029.
Jolivet, L., Goffé, B., Monié, P., Truffert-Luxey, C., Patriat, M., Bonneau, M., 1996. Miocene detachment in Crete and exhumation P-T-t paths of high-pressure metamorphic rocks. Tectonics 15, 1129–1153. https://doi.org/10.1029/96TC01417.
Jones, R.E., Kilikoglou, V., Olive, V., Bassiakos, Y., Ellam, R., Bray, I.S.J., Sanderson, D.C. W. 2007. A new protocol for the chemical characterisation of steatite – two case studies in Europe: the Shetland Islands and Crete. J. Archaeol. Sci., 626–641; doi.org/10.1016/j.jas.2006.07.002.
Klemm, R., Klemm, D.D., 2008. Stones and Quarries in Ancient Egypt. The Trustees of the British Museum Press, London, UK.
Koepke, J., Seidel, E., Kreuzer, H., 2002. Ophiolites on the southern Aegean islands Crete, Karpathos and Rhodes: Composition, geochronology and position within the ophiolite belts of the Eastern Mediterranean. Lithos 65, 183–203. https://doi.org/10.1016/S0024-4937(02)00165-2.
Kouka, O., 2009. Third Millennium BC Aegean Chronology: Old and New Data under the Perspectives of the Third Millennium AD. In: Manning, S.W. and Bruce, M.J. (Eds.), Tree-Rings, Kings, and Old World Archaeology and Environment: Papers Presented in Honor of Peter Ian Kuniholm, Oxford and Oakville, pp. 133–149.
Krzyszkowska, O., 2018. Materials, motifs, and mobility in Minoan glyptic. In: Proceedings of the 12th International Congress of Cretan Studies, 21–25 September 2016, Herakleion, pp. 1–17. https://12iccs.proceedings.gr/en/proceedings/category/38/32/368.
Lazzarini, L., 2001. I vasi in pietra minoici di Festòs: primi dati sulla natura e provenienza dei materiali lapidei. In: I Cento Anni dello Scavo di Festòs (Roma, 13–14 dicembre 2000), Atti dei Convegni Lincei 173. Accademia Nazionale dei Lincei, Rome, pp. 575–596.
Lazzarini, L., 2002. A new grey marble from Gortyna (Crete) used in Greek and Roman antiquity. In: Lazzarini, L. (Ed.), Interdisciplinary Studies on Ancient Stone: ASMOSIA VI. Proceedings of the Sixth International Conference of Association for the Study of Marble and Other Stones in Antiquity, Venice, 15-18 June 2000. Bottega d' Erasmo – Aldo Ausilio Editore, Padova, pp. 227–232.
Lazzarini, L., Markopoulos, T., Palio, O., 2002. The stones of the Minoan vases of Phaestos: preliminary results concerning their nature and origin. In: Lazzarini, L. (Ed.), ASMOSIA VI. Proceedings of the Sixth International Conference of the Association of the study of marble and other stones in antiquity, Venice, 15-18 June 2000. Bottega d' Erasmo – Aldo Ausilio Editore, Padova, pp. 443–451.
Legarra Herrero, B., 2011. The Secret Lives of the Early and Middle Minoan Tholos Cemeteries: Koumasa and Platanos. In: Murphy, J.M.A. (Ed.), Prehistoric Crete. Regional and Diachronic Studies on Mortuary Systems, INSTAP Academic Press, Philadelphia, pp. 49–84.
Legarra Herrero, B., 2014. Mortuary Behavior and Social Trajectories in Pre- and Protopalatial Crete (Prehistory Monographs 44). INSTAP Academic Press, Philadelphia.
Marthari, M., 2017. Cycladic figurines in settlements: the case of the major EC II settlement at Skarkos on Ios. In: Marthari, M., Renfrew, C., Boyd, M.J. (Eds.), Early Cycladic Sculpture in Context. Oxbow Books, Oxford and Philadelphia., pp. 119–164.
Meinhold, G., 2010. Rutile and its applications in earth sciences. Earth-Sci. Rev. 102, 1–28. https://doi.org/10.1016/j.earscirev.2010.06.001.
Morero, É., 2016a. Les techniques de fabrication de la vaisselle de pierre de Myrtos-Pyrgos. Bulletin de Correspondence Hellénique 138, 329-360.
Morero, É., 2016b. Méthodes d'analyse des techniques lapidaires. Les vases de pierre en Crète à l âge du Bronze (IIIe–IIe millénaire av. J.-C.). Publications de la Sorbonne, Paris.
Murphy, J.M.A., 2011. Landscape and Social Narratives: A Study of Regional Social Structures in Prepalatial Crete. In: Murphy, J.M.A. (Ed.), Prehistoric Crete. Regional and Diachronic Studies on Mortuary Systems, INSTAP Academic Press, Philadelphia, pp. 23–47.
Palio, O., 2003. Vasi in pietra dai livelli MM II del "Settore Nord-Est" di Haghia Triada". Creta Antica 4, 329–432.
Palio, O., 2008. I vasi in pietra minoici da Festòs. Bottega d' Erasmo – Aldo Ausilio Editore, Padova, Italy.
Palio, O., Cucuzza, N., 2018. Between memory and reuse in Late Minoan III Mesara: the stone vessels at Kannià. In: Borgna, E., Caloi, I., Carinci, F.M. and Laffineur, R. (Eds.), MNHMH/MNEME: past and memory in the Aegean Bronze Age: proceedings of the 17th International Aegean Conference, University of Udine, Department of Humanities and Cultural Heritage, Ca' Foscari University of Venice, Department of Humanities, 17-21 April 2018 (AEGAEUM 43). Peeters, Leuven – Liège, pp. 473–479.
Panagiotopoulos, D., 2015. Μινωική Κουμάσα: Ανασυνθέτοντας την ιστορία ενός μεθορίου κέντρου της νότιας Κρήτης. In: Karanastasi, P., Tzigounaki, A. and Tsigonaki, C. (Eds.), Archaeological work in Crete 3: proceedings of the 3rd meeting, Rethymnon, 5-8 December 2013. Rethymnon, pp. 227–238.
Papliaka, Z.E., Philippidis, A., Siozos, P., Vakondiou, M., Melessanaki, K., Anglos, D., 2016. A multi-technique approach, based on mobile/portable laser instruments, for the in situ pigment characterization of stone sculptures on the island of Crete dating from Venetian and Ottoman period. Heritage Science 4:15; doi.org/10.1186/s40494-016-0085-2.
Prinsloo, L.C., Colomban, P., Brink, J.D., Meiklejohn, I., 2011. A Raman spectroscopic study of the igneous rocks onMarion Island: a possible terrestrial analogue for the geology on Mars. J. Raman Spectrosc. 42, 626–632. https://doi.org/10.1002/jrs.2756.
Rahl, J., Fassoulas, C., Brandon, M.T., 2004. Exhumation of high-pressure metamorphic rocks within an active convergent margin, Crete, Greece: A field guide. 32nd International Geological Congress, Florence, Italy, 20–28 August 2004 (Field Trip Guide Book no 2, B32), Rome.
Relaki, M., 2012. In: Back to the Beginning. Reassessing Social and Political Complexity on Crete during the Early and Middle Bronze Age. Oxbow Books, Oxford and Oakville, pp. 290–324.
Relaki, M., Tsoraki, C., 2017. Variability and differentiation: A first look at the stone vase assemblage in the Petras cemetery. In: Tsipopoulou, M. (Ed.), Petras Siteia. The Pre- and Proto-palatial cemetery in context. The 2nd International Petras Symposium, The Danish Institute at Athens, 14-15 February 2015, 159-178 (Monographs of the Danish Institute at Athens, 20). The Danish Institute at Athens, Athens.
Rinaudo, C., Gastaldi, D., Belluso, E., 2003. Characterization of chrysotile, antigorite and lizardite by FT-Raman spectroscopy. The Canadian Mineralogist 41, 883–890. https://doi.org/10.2113/gscanmin.41.4.883.
Rruff - an integrated database of Raman spectra, X-ray diffraction and chemistry data for minerals, http://rruff.info.
Schoep, I., 2002. Social and Political Organization on Crete in the Proto-palatial period: the case of Middle Minoan II Malia. J. Mediterranean Archaeology 15, 101–132. https://doi.org/10.1558/jmea.v15i1.101.
Schörgendorfer, A., 1951. Ein mittelminoisches Tholosgrab bei Apesokari. In: Matz (Ed.), Forschungen auf Kreta 1942, Berlin, pp. 13–22.
Seidel, E., Okrusch, M., Kreuzer, H., Raschka, H., Harre, W., 1981. Eo-alpine metamorphism in the uppermost unit of the Cretan nappe system - Petrology and geochronology - Part 2. Synopsis of high-temperature metamorphics and associated ophiolites. Contrib. Mineral. Petrol. 76, 351–361.
Seidel, E., Kreuzer, H., Harre, W., 1982. A Late Oligocene/Early Miocene high pressure belt in the External Hellenides. Geol. Jahrb. 23, 165–206.
Shelmerdine, C.W., 2008. Background, sources, and methods. In: Shelmerdine, C.W. (Ed.), The Cambridge Companion to the Aegean Bronze Age. Cambridge University Press, Cambridge, pp. 1–18.
Smith, D.C., 2006. A review of the non-destructive identification of diverse geomaterials in the cultural heritage using different configurations of Raman spectroscopy. In: Maggetti, M. and Messiga, B. (Eds.), Geomaterials in Cultural Heritage (Geological Society, London, Special Publications, 257). London, pp. 9–32.
Smith, G.D., Clark, R.J.H., 2004. Raman microscopy in archaeological science. J. Archaeol. Sci. 31, 1137–1160. https://doi.org/10.1016/j.jas.2004.02.008.
Stampolidis, N.C., Sotirakopoulou, P., 2011a. Early Cycladic Period: Introduction. In: Şahoğlu and Sotirakopoulou (Eds.), ACROSS. The Cyclades and Western Anatolia during the 3rd Millennium BC. Sabancı Üniversitesi, Sakıp Sabancı Müzesi, Istanbul, pp. 18 – 24.
Stampolidis, N.C., Sotirakopoulou, P., 2011b. Early Cycladic stone artefacts and idols. In: Şahoğlu and Sotirakopoulou (Eds.), ACROSS. The Cyclades and Western Anatolia during the 3rd Millennium BC. Sabancı Üniversitesi, Sakıp Sabancı Müzesi, Istanbul, pp. 64 – 84.
Stos-Gale, Z.A., Gale, N.H., 2003. Lead isotopic and other isotopic research in the Aegean. In: Foster, K.P. and Laffineur, R. (Eds.), METRON: Measuring the Aegean Bronze Age (AEGAEUM 24). Liège and Austin: Université de Liège and University of Texas at Austin, pp. 83–101.
Tambakopoulos, D., Maniatis, Y., 2017. Shedding new light on the Early Bronze Age marble figurines from Crete: Types and sources of marble. In: Stampolidis, N., Sotirakopoulou, P. (Eds.), Cycladica in Crete. Cycladic and Cycladicizing figurines within their archaeological context. Proceedings of the International Symposium Museum of Cycladic Art, Athens, 1 – 2 October 2015. Cycladic Museum of Art, Athens, pp. 501–516.
Tortorici, L., Catalano, S., Cirrincione, R., Tortorici, G., 2012. The Cretan ophiolite-bearing mélange (Greece): A remnant of Alpine accretionary wedge. Tectonophysics 568–569, 320–334. https://doi.org/10.1016/j.tecto.2011.08.022.
Triantaphyllou, S., 2016. Staging the manipulation of the dead in Pre- and Protopalatial Crete, Greece (3rd-early2nd mill. BC): from body wholes to fragmented body parts. Journal of Archaeological Science. Reports (Special Issue for Funerary Taphonomy) 10, 769–779.
Triantafyllou, S., 2018. Managing with death in Prepalatial Crete: the evidence of the human remains. In: Relaki, M., and Papadatos, Y. (Eds.), From the Foundations to the Legacy of Minoan Archaeology. Studies in honour of Professor Keith Branigan (Sheffield Studies in Aegean Archaeology). Oxbow Books, Oxford and Philadelphia, pp. 141–166.
Tsikouras, V., forthcoming. Petrographic classification of stone objects from Apesokari through Raman spectroscopy. In: Flouda, G., An archaeological palimpsest. Tholos Tomb A and Habitation at Apesokari Mesara. INSTAP Academic Press, Philadelphia.
Tziligkaki, E.K., 2007. In quest of raw materials for the Cycladic figurines in Crete. In: Stampolidis, N., Sotirakopoulou, P. (Eds.), Cycladica in Crete. Cycladic and Cycladicizing figurines within their archaeological context. Proceedings of the International Symposium Museum of Cycladic Art, Athens, 1 – 2 October 2015. Cycladic Museum of Art, Athens, pp 453–498.
Vandenabeele, P., Edwards, H.G.M., Moens, L., 2007. A decade of Raman spectroscopy in art and archaeology. Chem Rev. 107, 675–686; doi.org/10.1021/cr068036i.
Vasilakis, A., 2017. Cycladicizing and Cycladic figurines from south-central Crete. In: Marthari, M., Renfrew, C., and Boyd, M.J. (Eds.). Early Cycladic Sculpture in Context. Oxbow Books, Oxford and Philadelphia, pp. 291–297.
Vavouranakis, G., 2015. The EM-MM tholos tomb B at Apesokari, Mesara: The results of the works in 2012 and 2013. In: Karanastasi, P., Tzigounaki, A. and Tsigonaki, C. (Eds.), Archaeological work in Crete 3: proceedings of the 3rd meeting, Rethymnon, 5-8 December 2013. Rethymnon, pp. 217–226.
Vickers, M., Gill, D., 1994. Artful Crafts. Ancient Greek Silverware and Pottery. Clarendon Press, Oxford.

Warren, P., 1967. A Stone Vase Maker's Workshop in the Palace at Knossos. Ann. Br. School at Athens 62, 195–201. https://doi.org/10.1017/S006824540001412X.
Warren, P.M., 1969. Minoan Stone Vases. Cambridge University Press, Cambridge, UK.
Warren, P., 2017. Egyptian alabaster and Minoan (Bronze Age Cretan) stone vases. Marmora 13, 11–24. https://doi.org/10.19272/201701401001.
Westlake, P., Siozos P., Philippidis A., Apostolaki C., Derham B., Terlixi A., Perdikatsis V., Jones R., Anglos D., 2012. Studying pigments on painted plaster in Minoan, Roman and Early Byzantine Crete. A multi-analytical technique approach. Anal. Bioanal. Chem. 402 1413–1432; doi.org/10.1007/s00216-011-5281-z.
Whitelaw, T.M. 2017. The development and character of urban communities in Prehistoric Crete in their regional context: a preliminary study. In: Letesson, Q. and Knappett, C. (Eds.), Minoan Architecture and Urbanism: New Perspectives on an Ancient Built Environment. Oxford University Press, Oxford. pp. 114–180.
Wilson, D., 2008. Early Prepalatial Crete. In: C.W. Shelmerdine (Ed.), The Cambridge Companion to the Aegean Bronze Age. Cambridge University Press, Cambridge, pp. 77–104.
Wojcieszak, M., Wadley, L., 2019. A Raman micro-spectroscopy study of 77,000 to 71,000 year old ochre processing tools from Sibudu, KwaZulu-Natal, South Africa. Herit Sci 7, 24; doi.org/10.1186/s40494-019-0267-9.
Xanthoudides, S. 1924. The Vaulted Tombs of Mesará: an Account of some Early Cemeteries of Southern Crete. Hodder & Stoughton, London.